Universitetet i Stavanger

FACULTY OF SCIENCE AND TECHNOLOGY

MASTER'S THESIS

Study program/specialization: Petroleum Engineering / Drilling Engineering	Spring semester, 2018 Open/~~Confidential~~
Author: Kamil Przymuszala	..... (signature of author)
Program coordinator: Mohsen Assadi Supervisors: Alireza Zare, Milad Khatibi	
Title of master's thesis: Numerical simulation of flows in concentric and eccentric annulus – relevant to geothermal wells	
Credits: 30	
Keywords: Geothermal energy Fluid dynamics Heat transfer Heat transfer in a wellbore	Number of pages: .....71..... + ~~supplemental material/other:....~~ Stavanger, 06.07.2018 date/year

Title page for Master's Thesis
Faculty of Science and Technology

Abstract

At the end of 20th century, the utilization of geothermal energy has increased by 150% forming a solid industry of relevant importance on global markets (Dickson & Fanelli, 2004). According to numerous analyses, this type of energy exploitation has a strong forecast of development in the future. High potential of progress is associated with complex studies to ensure the feasibility, safety and profitability of the investments.

Numerical simulation of flows in geothermal exploitation is an essential tool to establish adequate results. The assessment of this process is a key factor for preparing schemes providing high overall efficiency (Vasini et al., 2017). Determining the most favorable parameters and approaches is the subject of plenty studies in the field of geothermal energy.

This work analyzes the concept of geothermal energy and heat transfer in general, and in the wellbore. Furthermore, it investigates application of separate turbulence models on flow in concentric and eccentric annulus. Different assembly of pipes require adjusting diverse approaches to achieve finest results. When chosen models work for theoretical configurations, they do not automatically comply for the field cases. As for the eccentricity, the simulation shows valuable data of how the flow behaves in irregular, but very common position.

Obtained results satisfy the benchmarks stated in the preceding researches. For instance, the thermal structures are more aroused near the outer wall of the assembly, than closer to the inner pipe. This outcome might be implemented in analyzing vortex generations in the annuli. Moreover, the study defines the dependence of heat transfer rate on the pipe materials.

Conducted research might be used as an initial and easy to comprehend overview of the heat transfer phenomena in geothermal energy exploitation.

Acknowledgments

I would like to thank all my friends and family who have supported me during my studies at University of Stavanger. Because of them, this time was a remarkable and worthwhile challenge that I am proud to have completed.

I would like to address my gratitude to my supervisors – Alireza Zare and Milad Khatibi. Time spent on this project was not short and simple, but with your guidance and patience I was able to deliver this thesis.

I want to especially point out the encouragement I have received from my longtime mentor Marek, who made it all possible. I highly appreciate your time, advice and effort you put to help me find my educational and professional path.

Table of contents

List of figures

List of tables

Abbreviations

API	American Petroleum Institute
BC	Boundary condition
BHE	Borehole heat exchanger
BOP	Blow out preventer
CFD	Computational fluid dynamics
CHP	Combined heat and power
CO_2	Carbon dioxide
DNS	Direct numerical simulation
DSM	Design simulation model
EGS	Enhanced geothermal system
ESP	Electric submersible pump
EVM	Eddy-viscosity model
FVM	Finite volume method
GUI	Graphical user interface
H_2S	Hydrogen sulfide
HDR	Hot, dry rock
LES	Lage eddy simulation
NLEVM	Non-linear eddy-viscosity model
PRESTO	Pressure staggered option
RANS	Reynolds-average Navier-Stokes
RNG	Renormalization group
ROP	Rate of penetration
RSM	Reynolds stress model
RSTM	Reynolds-stress transport model
SI	International system of units
SOC	second-order closure model
SST	Shear stress transport
TES	Thermal energy storage
TKE	Turbulence Kinetic Energy
UCS	Union of Concerned Scientists

1. Introduction

Energy industry is considered one of the most important sectors that establishes a background for majority of diverse businesses. In 2016, according to Advanced Energy Economy association, 'Advanced Energy' field was worth 1,4 trillion US dollars globally with a stable forecast of growth. Along with that progress, Renewable Energy strengthens its position in the fastest way compared to other sectors.

One of the significant parts of the Renewable Energy sector is a geothermal energy and it is the only 'energy source independent of solar radiation and/or the gravitational attraction of the sun and moon' (Younger, 2014). Geothermal energy is expected to grow essentially in upcoming years due to countries national policies of changing energy mixes and meeting climate agreements to lower CO_2 emissions, i.e. one of the most common geothermal plants type, a 'binary cycle power plant', has no harmful output to the atmosphere, just water vapor.

So far, the annual growth of geothermal energy importance averages at around 5%, overtaken by the development of photovoltaic and wind industries. Carr-Cornish and Romanach (2014) suggests that there are two reasons for this situation:

- uncertainties over resource availability in poorly-explored reservoirs,
- the cost profile, in which a large proportion of the full-lifetime costs of systems are concentrated in early-stage capital expenditure (capex).

Both issues are steadily addressed by further researches and operations and would definitely improve over the next decades. Besides that, the Union of Concerned Scientists (UCS) notices that the amount of heat within 10 000 meters of Earth's surface contains 50 000 times more energy than all the oil and natural gas resources in the world. With such huge potential, the geothermal energy sector would become a major field and gain significance around the world.

It has been evaluated, that in some markets the cost of working geothermal plant declined by 50% since the 1980s. This gives solid background for forecasts suggesting that the energy from geothermal plants will be as cheap as from other resources, like fossil fuels with much higher carbon footprint.

Intergovernmental Panel on Climate Change predicts, that the geothermal energy will account for at least 4% of the world's power supply. Other institutions foresee even larger share of the market.

1.1.Background of the problem

Neto et al. (2011) investigated the flows occurring in concentric and eccentric annuli with movement (or without) of inner cylinder that transmits power. This study reflects problems existing in Petroleum Industry while performing drilling operations. They prepared CFD

simulations for axial and tangential velocities and compared with data obtained by the Nouri et al. (1993) and Nouri and Whitelaw, 1997).

Heat transfer behavior in heat exchangers was characterized by Kumar et al. (2006). Their work covered numerous parameters regarding thermal development for various flow rates in inner-coiled tube and in the annulus region. Received solutions were close to numerical predictions based on preceding researches.

Chung et al. (2002, 2003) conducted two major studies on numerical simulation for concentric annular pipe flow, regarding the flow field and heat transfer. Their work provided insight into the general problem of fully developed turbulent shear flows. Moreover, the numerical results demonstrate that the turbulent thermal structures are more stimulated near the outer wall, than those near the inner wall. This concept could be implemented to various vortex generation processes between the walls.

Busch et al. (2016) prepared a benchmark specification for cuttings transport with reference to drilling operations. Set parameters are gathered with respect to operations performed on Norwegian Continental Shelf. It gives valuable input on how to standardize following projects.

1.2.Statement of the problem (Research question)

With a significant increase of geothermal energy exploitation over the years, aligned with the development of drilling techniques, the importance of an adequate simulation of production scheme becomes essential.

Franco and Vaccaro (2014) pointed out the necessity of numerical simulation for the geothermal reservoir assessment, which can be obtained by consistent investigation of generation stage. As in case of usual hydrocarbons exploitation, several factors can affect the production phase.

The main issue, that needs to be addressed, is how the flow of medium in the annulus is influenced by the eccentricity of the inside pipe.

1.3.Objectives and scopes of the study

The objectives and scopes for this study are:

- Provide analysis on geothermal energy, geothermal wells and heat transfer in the annulus
- Conduct simulations of flows in concentric and eccentric annuli using Ansys Fluent
- Demonstrate various turbulence models with Reynolds Average Navier-Stokes approach
- Identification of heat transfer changes due to materials of pipes variations

1.4.Approach

This study was carried out using ANSYS-FLUENT software package. The benchmark simulation, geometry and boundary conditions were related to paper published by Neto et al. (2011) to assure the relevance and accuracy of the investigations. Further cases were conducted on industry standards and real-life examples to add supplementary value to the analysis recognized in official preparations for geothermal exploitation.

1.5.Significance of the study

The work of projecting separate turbulence models of flows in annuli of concentric and eccentric wells gives a brief overview of geothermal exploitation. Analyzing several conditions of fluid dynamics is essential for proper understanding of this issue. This research provides farther data on benchmark, sample cases and on examples used normally in the geothermal business.

The overall objective of the investigation of diverse turbulence models for several geometric arrangement of annulus assemblies is to provide improved information of how the heat transfer behaves under particular conditions.

2. Theory

2.1.Geothermal energy

Geothermal energy is a thermal energy generated and stored in the Earth. It is extracted from crust and has approximately stable temperature. In general, geothermal fluids are steam or hot water that can serve not only in electricity and heat generations, but also in projects relevant to industries like agriculture or food processing. Geothermal energy is classified as a renewable energy resource that is naturally replenished, and their usage takes place with no major harm (no combustion of fuel) to the environment (Petrică, 2016).

By the reason of much hotter Earth's interior than its surface, energy circulates constantly from the deep formations up to the exterior parts. This process is commonly named as a terrestrial heat-flow (Toth, 2017). Major foster of development has been seen in the last decades due to significant improvements of deep drilling techniques that originally contributed to oil & gas explorations. The equipment and practices have many similarities between those two sectors (Petrică, 2016).

The essence of geothermal energy is to absorb the heat from the rock by transporting water to the surface and convert it to electricity and heat for purposes standing economic reasons (Gallup, 2009 no. 24). It is especially suited to CHP applications (combined-heat-and-power) (Heberle & Brüggemann, 2014). As both objectives are fulfilled, the general efficiency of the plant is much higher than for other means of energy. Moreover, the geothermal energy ventures have huge capacity factors exceeding 90% (sometimes even 95%). Thus, they can operate constantly producing large amounts of energy and heat (Younger, 2015).

Another rapidly-growing production technology involves exploiting the energy content of near-surface regions by using shallow borehole heat exchangers and heat pumps (Toth, 2017). What is more, further studies are also conducted on developing thermal energy storage (TES) to manage the facility's energy production and use in time, temperature or power (Rapantova et al., 2016).

2.1.1.Geothermal system and reservoir

Hochstein (1990) noticed that the term 'geothermal system' was used to characterize naturally convecting waters in the upper crust of the earth, which in confined space distribute heat from a source to a heat sink, usually the free surface, but the phrase was later broadened to any resource of heat that extraction would be economically reasonable. At the same time, he described the geothermal reservoir as a 'volume of rocks from which heat can be extracted'. It is normally surrounded by colder rocks connected to it hydraulically. Thus, water moves from them (recharge) to the reservoir. Here geothermal fluids, which have higher temperature, move to discharge area affected by the buoyancy forces. For a better understanding of the issue, the geothermal system in terms of geological aspects describes

the reservoir, heat source, natural discharge and surrounding rocks from where the fluids move both ways (inside and outside towards the reservoir). In some cases, the exploitation could only happen by artificial operation like injection of cold water and in others it would induced natural recharge. Those terms have not changed since then and are officially used in international nomenclature.

Faust and Mercer (1979) classified potential sources of geothermal energy into following systems:

- Hydrothermal – heat sources such as magmatic intrusions that lies on shallow depths of the surface area. They transfer the heat to a porous rock and the fluid within by conductive and convective processes. This can be classified further with liquid or vapor dominated systems (White et al., 1971),

- Geopressured – system, where fluid it cornered in permeable sedimentary rocks that are covered by a low permeable rock layer and exposed to high temperature and pressure, categorized as static,

- Hot, Dry Rock (HDR) – low-permeable hot igneous rocks that work analogously to hydrothermal systems. An injection well transfers cold fluid down through a drilled and completed well to formations generating heat. Absorbed heat is transported via heated fluid along the production well to the surface.

At the same time Hochstein (1990) uses a simplest classification of the reservoirs – in terms of their average temperature:

- Low temperature resources – temperature in economic wells is less than 125^{o}C,
- Intermediate temperature resources – temperature allocates between 125^{o}C and 225^{o}C,
- High temperature resources – temperature in economic wells exceeds 225^{o}C.

Williams et al. (2011) brought together the most common ways of categorization and the method made by Hochstein was suggested as an arbitrary example in many articles and projects. Nonetheless, they also pointed out arrangement introduced by Sanyal (2005). The geothermal systems were separated to six diverse groups based on their temperature (plus one special class of steam fields), but it has not become that universal.

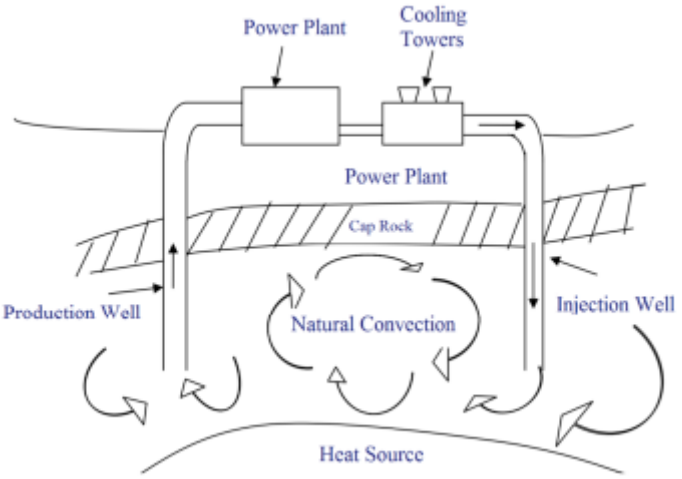

Figure 2-1. Scheme of a common geothermal system (Ganguly and Kumar, 2012).

2.1.2.Geothermal fluid

Official definition of 'geothermal fluid' specifies that it is a liquid, steam and gas together or each element solely. The state of the fluid (liquid or vapor) lean on the temperature and pressure of the reservoir. During the fluid movement from the source to the surface, it is characterized as a two-phase flow. Single phase flow of water rarely occurs.

Geothermal fluids may contain other components, usually carbon dioxide, methane and hydrogen, less frequently nitrogen and sulfide. Those gases are transferred to the steam phase upon boiling, because molecules tend to reside in the steam (Þórhallsson, 2011).

Þórhallsson (2011) points out that geochemists identified more than 20 chemical ratios and species governed by the temperature in potential geothermal reservoirs. Analysis of those elements is a relevant procedure that can help predict temperature and wealth of specific basin. At the same time generation of this energy demands complex production units to ensure safety and quality of the final product.

With constant development of the geothermal technology, other working fluids are considered instead of water. Pan et al. (2016) investigated advantages and disadvantages of using CO_2 as an operating mean. Major strengths of this idea are: lower external pumping energy because of low viscosity of the fluid, increased buoyancy effect due to high compressibility and expansivity enabling natural flow from high pressure injection well to low pressure production one. At the same time this method carries problems, like small heat capacity, which reduces the amount of heat that can be brought by one unit of fluid.

2.1.3.Environmental risks

As mentioned in the previous section, geothermal fluids contain various minerals and elements that can be unsafe for mankind, agriculture or wildlife. For example, fluids with high

temperature cause risks to vegetation and aquifers, since 'the quantity of dissolved solids increase substantially with temperature' (DiPippo, 2016).

Geothermal exploitation without proper integrity control would usually end up with fluids spilled to aquifers and groundwater. Migration from the reservoir along the poor-quality casing or cement in wellbore can carry heavy metals existing in soils. The geological aspects that could cause problems are related to the process of drilling – encountering swelling clays, highly permeable layers, unconsolidated formations and differential sticking (Lentsch et al., 2015).

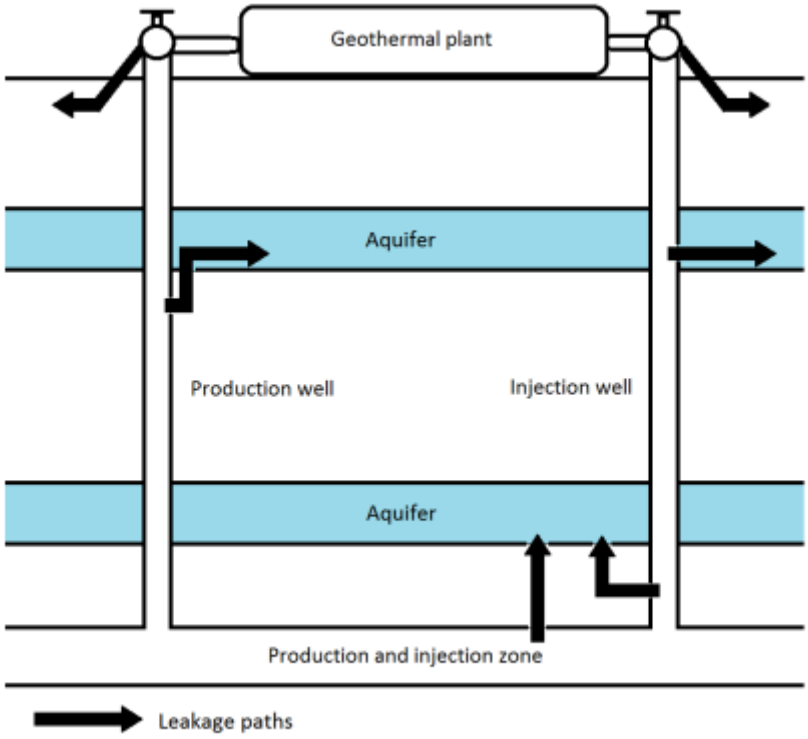

Figure 2-2.Hypothetical leakage paths. Adapted from Summers et al. (1980).

2.2.Geothermal wells

Geothermal wells are drilled and completed in a similar way to those exploring oil & gas reservoirs (Ikenwilo et al., 2016). With recent development of geothermal sector, deep wells have become a requirement, but the overall cost is 2-5 times greater of comparable depths in this case (Teodoriu & Falcone, 2009; Augustine et al., 2006). Moreover, the drilling costs dominate the total capital investment (Thorsteinsson et al., 2008).

Wells enabling geothermal production are uneasy to categorized because of the customize design fitting individual conditions, but Teodoriu and Falcone (2009) suggest following groups that could be compared with petroleum boreholes:

- Wellhead and surface equipment are excluded,
- Tubulars, connections, and well integrity factors are accounted for,
- Three typical well completions are assumed, representative of a geothermal producing well, a deep gas well and a heavy oil producer.

Augustine et at. (2006) Stated that drilling for geothermal reservoirs cause more challenges than for petroleum basins. Heat bearing formations are usually igneous or metamorphic, while oil & gas are mainly sedimentary. This leads to significant decrease of ROP because of more abrasive rocks and it transfers to higher number of bits needed to perform drilling operations. Thus, geothermal exploration also has managed to improve the petroleum sector (Carden et al., 1983).

2.2.1.Well design

Prior section put a light on the analogy between geothermal and petroleum wells. This applies in the well construction operations as well. Petrică (2016) categorized the process into five phases:

- Preliminary well design,
- Detailed well design,
- Preparation of drilling program,
- Execution of well program,
- Analysis and improvement of performance.

At this stage the well design requires same parameters for both industries. Several areas need to be examined to prepare construction that would fit environmental and engineering conditions. Having sufficient input data, the works can start from casings setting depths, drill string components, casing design, cementing program etc. Serpen, and Başel (2015) examined that it is more advantageous to drill geothermal wells with standard diameters rather than big ones.

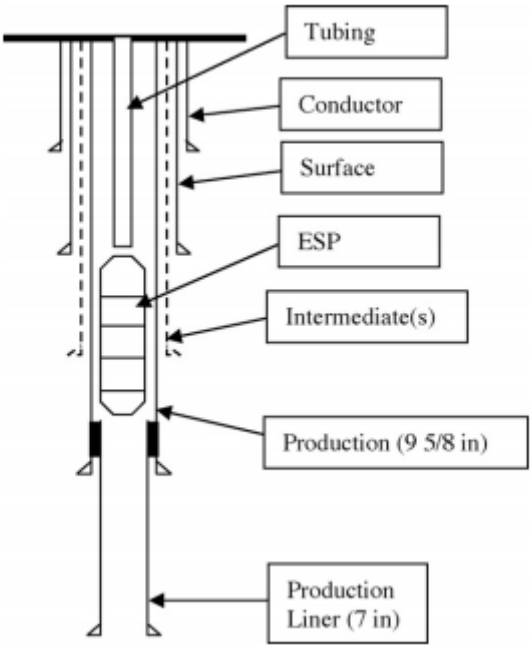

Figure 2-3. Example of completion diagram for a geothermal well requiring pumping. Adapted from Teodoriu and Falcone (2009).

2.2.2.Casings challenges

Geothermal drilling faces slightly different challenges compared to petroleum exploration. Hence, additional equipment is needed: rotating head, customize blow out preventer (BOP), cooling tower for mud, air compressors and separator for aerated drilling (Petrică, 2016). The occurrence of hole stability problems through loss of circulation or differential sticking is increased with low rate of penetration (due to abrasive rocks) that also requires precise mud weight determination.

Other problems that may occur with geothermal drilling (Lohne et al., 2016):

- Drill string vibrations caused by hard fractured rocks,
- Drill string stuck in the hole,
- Need of cementing caused by loss of circulation,
- Stuck of drill string requiring fishing operations,
- No returns while cementing the casing,
- Usual well control problems: kicks and blow-outs,
- High concentration of H_2S,
- Low ROP in abrasive rocks,
- Improper choice of drill bits slowing ROP,
- Equipment failures, personal mistakes etc.

Kaldal et al. (2015) investigated that geothermal wells experience much higher thermal stresses above the yield strength of casing due to considerable temperature change. This situation requires usage of stronger casing materials like K55, L80 and T95 (API grading). While planning a well the structural design needs to be evaluated, considering material strength reduction due to temperature, thermal expansion, wellhead pressure, corrosion or scaling (especially in wells deeper than 3000 m and with temperature higher than 120^{o}C [Wanner et al., 2017]).

2.3.Enhanced geothermal system

Naturally-occurring geothermal resources are limited on earth. They depend on considerable amounts of heat, fluid and low permeability levels in the reservoirs (Olasolo et al., 2016). To lower dependency on such systems, scientists proposed artificial solutions to maintain the potential of this energy source, calling it 'Enhanced Geothermal System' (or EGS). The concept of this alternative is about obtaining heat from a 'tight' rock with rather low permeability that was not fragmented naturally (Gallup, 2009). The usual working fluid is water pumped through zones of hot formations, so the heat exchange is possible.

2.4.Borehole heat exchangers

The mechanism of heat transfer (described in the next section) exists in many engineering applications. Specific device to carry out this process is called the heat exchanger. Among several fields of usage, the most common ones are: air-conditioning, waste heat recovery, petrochemical, food engineering and power production (Bahiraei et al., 2018). Popular, commonly used practice is an earth-air heat exchanger (EAHE) in building industry reducing the heating or cooling loads at the big scale (Estrada et al., 2018). The most elementary example is when hot and cold fluids move in the same or opposite direction in a concentric tube (Bergman et al., 2011). While both fluids enter at the same point, go together in the same direction and leave at another point, we can point out the parallel-flow. Meanwhile, the counterflow settlement means the opposite – fluids enter at different ends, flow in other directions and leave at different ends.

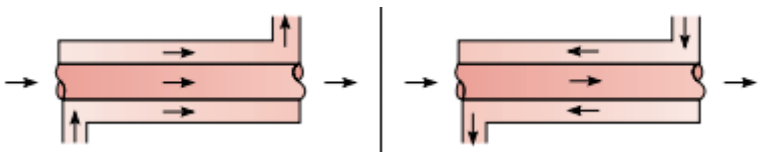

Figure 2-4. Example of concentric tube heat exchangers: parallel-flow (left) and counterflow (right) (Bergman et al., 2011).

Heat exchangers are also useful in all power and chemical facilities to recover waste heat previously released to atmosphere and now decreasing the consumption of primary energy source and costs in these units (Kayabasi & Kurt, 2018).

As it was described before, the most efficient geothermal exploitation method is by extracting groundwater from the reservoir, but if a large amount of it is exploited, it will cause major environmental problems like subsidence. Re-injecting the geothermal fluid is a must in dominant cases, but when the source occurs in sandstone layers, it is very challenging. To meet the environmental requirements while developing geothermal energy ventures, the borehole heat exchangers (or downhole heat exchangers) were introduced, as it only absorbs the heat, without extracting any fluids from the underground aquifer (Shi et al., 2018). As a typical heat exchanger, the one used in the geothermal exploitation consists of a series of tubes or a single U-tube. It is placed in the wellbore surrounded by the geothermal fluid. The working unit circulates through the BHE and derive the heat from the fluid. Shi et al. (2018) pointed out that this is a problematic process with natural convection (section 3.2.) caused by heat extraction of BHE and conduction (section 3.1.) of formation. Currently, it is investigated to replace he conventional working fluid (ethylene glycol/water mixture) with fluids containing nanoparticles (nanofluids) to enhance the heat transfer performance (Diglio et al., 2018).

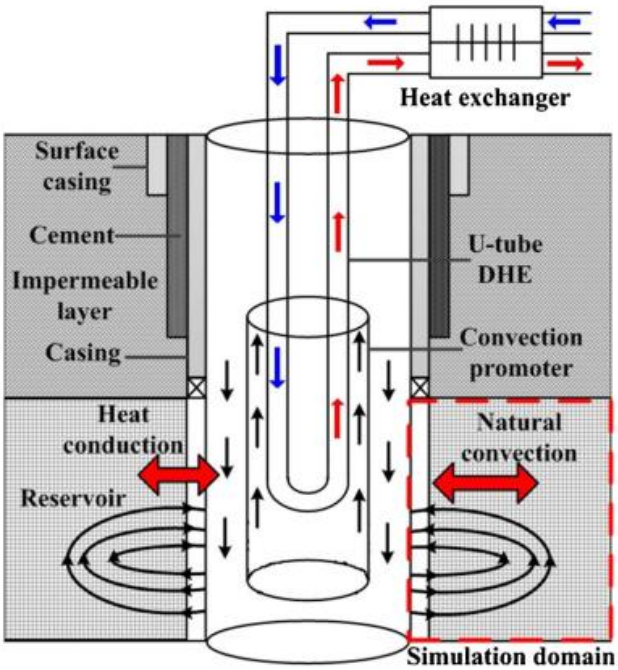

Figure 2-5. Example of borehole heat exchanger with a convection promoter (Shi et al., 2018).

2.5.Heat transfer

According to Bergman et al. (2011), heat transfer is a 'thermal energy in transit due to a spatial temperature difference'. Thus, whenever such diversity in a temperature of the systems exists, internal energy of the objects changes in respect to the first law of thermodynamics. Similarly, if there is no temperature difference, the heat exchange will not take place.

Different types of heat transfer processes are referred to as modes.

2.5.1.Conduction

According to literature, conduction means transfer of the energy due to interplay between particles of the material from more energetic ones, to less energetic fragments (Bergman et al., 2011). As high temperature correlates to high molecular energies, the conduction must occur because of constant interfering between neighboring molecules. Holman (2010) pointed out that the heat transfer rate per unit area is proportional to the normal temperature gradient:

$$\frac{q_x}{A} \sim \frac{\partial T}{\partial x}$$

Then, the proportionality constant 'k' must be introduced. It states the 'thermal conductivity' of the material. As can be noticed below, there is a minus sign in the equation, because it must fulfill the second principle of thermodynamics: 'heat must flow downhill on the temperature scale' (Holman, 2010).

$$q_x = -kA\frac{\partial T}{\partial x}$$

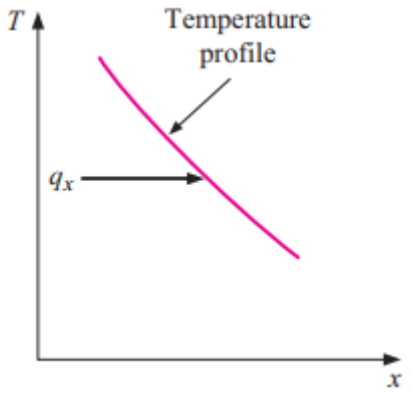

Figure 2-6. Direction of a heat flow (Holman, 2006).

In the given formula, the q_x is the heat transfer rate and $\partial T/\partial x$ is the temperature change in the direction of the transfer.

As the temperature change ($\partial T/\partial x$) is constant through the wall thickness (L), following formula is obtained:

$$\frac{dT}{dx} = \frac{T_2 - T_1}{L - 0} = \frac{T_1 - T_2}{L} = -\frac{\Delta T}{\mathrm{L}}$$

$$q_x = -\frac{k}{L}\Delta T$$

Later on, the heat flux equation is multiplied by the plane wall are to receive the heat rate by conduction for plane wall.

$$Q = -\frac{kA}{L}\Delta T$$

To analyze the wellbore example of production tubing, where the transfer happens in a cylindrical shell geometry, the inside and outside of a pipe must be introduced:

$$Q = -kA\frac{\mathrm{d}T}{\mathrm{dr}} = -k(2\pi rL)\frac{dT}{dr}$$

$$Q = \frac{2\pi Lk(T_1 - T_2)}{\ln(\frac{r_2}{r_1})}$$

2.5.2.Convection

Convection mode consists of two separate processes. Other than transfer due to molecular movement (diffusion), energy is transmitted by advection – through fluid bulk motion if a temperature gradient is present. The total heat transfer happens because of superposition of energy transport (irregular motion of molecules) and by bulk motion of the fluid (Bergman et al., 2011). Convective heat transfer is categorized in two groups:

- Forced mode – fluid flow energetically passed by a surface, i.e. fan,
- Natural or free mode – temperature variation of the fluid provokes buoyancy effect through change of density, i.e. pot with heated water.

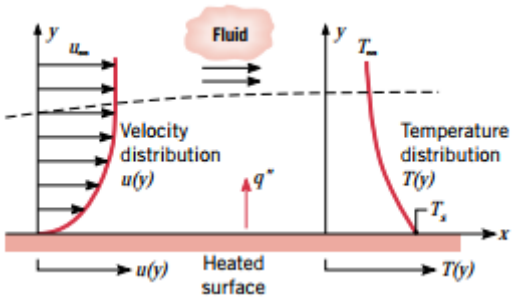

Figure 2-7. Convection heat transfer as a layer development (Bergman et al., 2011).

The heat flux in convection is described by following formula:

$$q = h(T_\infty - T_s) = h\Delta T$$

Where: T_s – temperature of the surface on which convection is considered

T_∞ – temperature of the free stream outside the velocity boundary layer

Above equation is also named as a Newton's law of cooling.

2.5.3.Radiation

While energy transfer in conduction and convection is through a material medium, heat in radiation does not require it and it transmits most efficiently over regions with perfect vacuum. In general, this is called electromagnetic radiation, but when caused by the temperature difference – thermal radiation (Holman, 2010). The emission is attributed to differences 'in the electron configurations of the constituent atoms or molecules' (Bergman et al., 2011). The ideal heat exchanger is a blackbody and energy which is emitted from it, is given by the Stefan-Boltzmann law of thermal radiation.

2.5.4.Thermal resistance

While considering the conduction of heat, electricity conduction analogy is used to describe the process of heat transfer through several layers of matter. The Ohms law characterizes the resistance of electricity conduction:

$$R = \frac{V}{I}$$

Where: R – electrical resistance

V – voltage

I – electrical current

One dimensional heat transfer can be compared as the heat flux (q) correlates to an electrical current.

$$R_{conduction} = \frac{\Delta T}{Q} = \frac{L}{kA}$$

$$Q = \frac{1}{R_{conduction}} \Delta T$$

In electricity, the resistance of electrical circuit in a series is just a sum of individual resistances of the components. In heat transfer, the thermal resistances (liquid or solid matters) also affect the rate of it. The value of heat transfer also depends on the thermophysical parameters of the materials in the system and the medium that transfers the heat.

If no storage of the energy in the system is assumed (and no additional generation) the heat transfer is constant. The conduction through solid materials is given by the formula:

$$Q = \frac{T_{s,1} - T_{s,2}}{L/kA}$$

Moreover, the heat transfer in the system becomes:

$$Q = \frac{T_{\infty,1} - T_{\infty,2}}{R_{total}}$$

and the total thermal resistance:

$$R_{total} = \frac{1}{h_1 A} + \frac{L}{kA} + \frac{1}{h_2 A}$$

Similarly, to electricity, the total resistance is a sum of the components' resistances.

$$R_{total} = \sum R_i = \frac{\Delta T}{Q} = \frac{1}{UA}$$

Where: U – overall heat transfer coefficient

2.6.Overall heat transfer coefficient

The heat transfer coefficient describes the rate of heat transferred from one medium to another one through a solid surface. The number could be defined for various cases, like for plane wall geometry or cylindrical geometry. Bergman et al. (2011) defined it as:

$$Q = UA\Delta T$$

Considering the thermal resistance example above, we obtain:

$$U = \frac{1}{R_{total}A}$$

Overall heat transfer coefficient for plane wall geometry (where the area 'A' is constant through the wall) becomes:

$$U = \frac{1}{R_{total}A} = [\frac{1}{h_1} + \frac{1}{k} + \frac{1}{h_2}]^{-1}$$

Now for the cylindrical geometry, the overall heat transfer coefficient is obtained in an analogous matter. The heat flow is considered radial across a pipe because of fluids with different temperatures moving along the pipe's axial path inside and outside. The conductive heat transfer is:

$$Q = \frac{2\pi Lk\Delta T}{\ln(\frac{r_2}{r_1})}$$

And the resistance has a form of:

$$R_{conduction} = \frac{\Delta T}{Q} = \frac{\ln(\frac{r_2}{r_1})}{2\pi r_1 Lk}$$

Next step is to introduce the total radial heat transfer through the pipe:

$$Q = \frac{\Delta T}{R_{total}} = \frac{T_{\infty,1} - T_{\infty,2}}{\frac{1}{2\pi r_1 Lh_1} + \frac{\ln(\frac{r_2}{r_1})}{2\pi Lk} + \frac{1}{2\pi r_2 Lh_2}}$$

The $T_{\infty,1}$ and $T_{\infty,2}$ parameters express the inside and outside average flow temperatures. If the pipe inside area is defined as a $A=2\pi r_1 L$, then the overall heat transfer coefficient U is:

$$U_1 = \frac{1}{R_{total}A} = [\frac{1}{h_1} + \frac{r_1 \ln(\frac{r_2}{r_1})}{k} + \frac{r_1}{r_2}\frac{1}{h_2}]^{-1}$$

If next layers are considered, the new resistance terms are added in an analogous matter.

2.7.Properties of heat transfer

2.7.1.Thermal conductivity

According to Bergman et al. (2011), thermal conductivity describes material's individual transport ability to conduct heat. It is included in Fourier's law (thermal conduction) and indicates the energy transfer rate in the diffusion process. Its value may change due to temperature and pressure of matter, as a reason of specific physical structure of the material.

Thermal conductivity is expressed by 'k' in the following formula:

$$k = -\frac{q_x}{\partial T/\partial x}$$

Where q_x states the heat flux and $\partial T/\partial x$ the temperature change over a distance. As can be noticed, the thermal conductivity increases with the heat flux raise. In general, it has a larger value for a solid than for a liquid or gas. This means that the energy transfer is less efficient in both fluid or gas states because of considerable intermolecular distance and random movement of particles. For solids, the driver for migration is lattice vibrational waves and mobility of free electrons.

In gases, thermal conductivity corresponds proportionally to gas density, mean molecular speed and usual distance a molecule covers before hitting another particle. For the fluids the background of conductivity is not properly examined (Bergman et al., 2011).

2.7.2.Specific heat capacity

The ability of the material to store heat as a kinetic (or vibrational) energy on an atomic level is referred to as specific heat capacity (c_p). There are several issues for a proper description of this term, i.e. electron distribution, lattice vibration spectrum or relations between molecules. The specific heat capacity is an intensive physical property, so it is independent of the system's size or the material volume present in it.

Specific heat capacity relates to the amount of energy needed to change the temperature of particular substance per unit of mass. In SI units it is expressed in $[\frac{J}{kg*K}]$.

Specific heat capacity cannot be confused with heat capacity describing the heat change in the system resulted in temperature difference.

2.7.3.Thermal diffusivity

Bergman et al. (2011) pointed out, that thermal diffusivity measures the capability of a material to 'conduct thermal energy relative to its ability to store thermal energy'. In a simple form it is a ratio between thermal conductivity to the heat capacity marked as:

$$\alpha = \frac{k}{\rho c_p}$$

This gives a value of the energy transfer rate through a material measured in SI units.

Higher values of α means that materials can respond quickly to the changes in the thermal surrounding, while small values imply that objects need more time to adjust to new thermal situation.

2.7.4.Viscosity

One of the most crucial parameters of a fluid is its viscosity as it is a measure of the resistance to the flow. The elements suspended in the fluid have influence on its behavior. When they are in the size of molecules, the system behaves as a Newtonian fluid. On the contrary unsymmetrical particles may result in non-Newtonian behavior. The viscosity of a fluid is given by its ratio of shear stress, τ (Pa), to the share rate, γ (1/s):

$$\mu = \frac{\tau}{\gamma}$$

To simplify, fluids are described by ideal theoretical models: Newtonian and Bingham plastic. For the first one viscosity is stable, regardless of different shear rates. For Bingham plastic the relation is not linear because the fluid must overcome an initial shear stress and yield point

to start movement. After passing the yield point, the behavior clarifies to a Newtonian mode.

2.7.5.Density

Density can be expressed in various ways depending on the structure of the material (homogeneous or heterogeneous). In general, it is defined as a ratio between substance's mass (m) to its volume (V). For porous media it is density calculated from the substance in the pore space adding the porous material, which can be defined as the bulk density.

$$\rho = \frac{m}{V}$$

Density is affected by the temperature and pressure. With the increase of pressure, the material is shrinking with the same mass, so the density grows. While increasing the temperature the volume expands thus there is a reduction in density.

2.8.Joule-Thomson effect

To understand one of the main drivers in the medium transfer along the production tubing in a well, the pressure loss concept must be introduced.

The simplest scenario considers steady state, Newtonian and incompressible flow over the small, differential fluid material dL. There is no inclination form the vertical position (θ=0) and no work was conducted over the system, while assuming the mechanical energy conservation over the element, the change in energy will be shown as:

$$\frac{dp}{\rho} + \frac{dv^2}{2} + gcos\theta dL = -f_D \frac{dL}{d} \frac{v^2}{2}$$

Where: p – pressure

ρ – fluid density

v – fluid velocity

g – standard gravity

f_D – Darcy friction factor

d – inner pipe diameter

Parts of the equation represent different elements of the whole process. Starting from left it is pressure, kinetic, potential and frictional energy changes through the fluid element. Looking for the pressure change over a certain distance (solving for $\frac{dP}{dL}$), the result is:

$$-\frac{dP}{dL} = \frac{f_D dv^2 \rho}{2d} + \rho v \frac{dv}{dL} + \rho g cos\theta$$

The final pressure loss of a fluid going upwards is expressed a sum of friction, momentum and static pressure losses.

$$(\frac{dP}{dL})_{Total} = (\frac{dP}{dL})_{Friction} + (\frac{dP}{dL})_{Momentum} + (\frac{dP}{dL})_{Static}$$

As the medium moves upwards to the surface, it experiences a pressure drop and a change of temperature. In case of a movement inside the tubing, the surrounding pressure decreases. This reaction is called Joule-Thomson effect, identified as:

$$\mu_{JT} = (\frac{\partial T}{\partial P})_H$$

Where: μ_{JT} – Joule-Thomson coefficient

H – the enthalpy of the process

2.9.Heat Transfer in a wellbore

In a case of a fluid filled wellbore, the heat transfer by radiation can be ignored due to the fact, that two other modes (convection and conduction) are the governing ones. Radiation heat transfer is used in the wellbore, where annulus is filled with gas (Zhou and Zeng, 2015).

2.9.1.Temperature

When considering the hot fluid transported through production tubing in a well, the temperature of the surrounding formation will change. The diffusion of heat in the geological formation is seen as a three-dimensional issue, but according to Hasan and Kabir (1991) if the symmetry over a heat source is assumed, this problem in a well can be managed as a two-dimensional example. Moreover, for further simplification, the small increase in the vertical direction can be neglected. Thus, the whole situation reduces to a one-dimensional case.

To present the issue described above, several assumptions must be stated: constant heat flow in the small section of a well, in a narrow time step. Hence, the problem is governed by partial differential equations in cylindrical coordinates:

$$\frac{\partial^2 T_e}{\partial r^2} + \frac{1}{r}\frac{\partial T_e}{\partial r} = \frac{c_e \rho_e}{k_e}\frac{\partial T_e}{\partial t}$$

Where: t – time

T_e – formation temperature at a time t

r – radial distance from the center of a well

c_e – specific heat capacity of formation

ρ_e – density of a formation

$\frac{c_e \rho_e}{k_e}$ – thermal diffusivity of a formation

For further calculations, the dimensionless radius and time must be introduced:

$$r_D = \frac{r}{r_{wb}}$$

$$t_D = \frac{\alpha_e t}{r_{wb}^2}$$

Where r_{wb} is a wellbore radius. Considering assumptions mentioned before, the formation temperature is constant at any depth:

$$\lim_{t \to 0} T_e = T_{ei}$$

T_{ei} is temperature distributed far away from the borehole and it does not change at the outer temperature boundary condition with the increase of a distance from the well:

$$\lim_{r \to \infty} \frac{\partial T_e}{\partial r} = 0$$

Next step is to introduce the heat flow rate from produced medium per unit length of the well:

$$Q = -\frac{2\pi k_e}{\omega}\frac{r \partial T_e}{\partial r}\Big|_{r=r_{wb}}$$

In this formula, ω expresses the mass flow rate of produced medium. With dimensionless components mentioned above, the main equations become:

$$\frac{\partial^2 T_e}{\partial r_D^2} + \frac{1}{r_D}\frac{\partial T_e}{\partial r_D} = \frac{\partial T_e}{\partial t_D}$$

$$\lim_{r_D \to \infty} \frac{\partial T_e}{\partial r_D} = 0$$

$$\frac{\partial T_e}{\partial r_D}\Big|_{r_D=1} = -\frac{\omega Q}{2\pi k_e}$$

Above equations can be solved with Laplace transform, so the interface temperature in a well is:

$$T_{wb} = T_{ei} + \frac{\omega Q}{\pi^2 k_e} I$$

$$I = \int_0^\infty \frac{1 - e^{-u^2 t_D}}{u^2} \frac{Y_1(u) - J_1(u)Y_0(u)}{J_1^2(u) + Y_1^2(u)} du$$

Where: u – indicator variable

J_0, J_1 – zero and first-order Bessel functions of first kind

Y_0, Y_1, - zero and first-order modified Bessel functions of first kind

This is how the dimensionless temperature is defined:

$$T_D = -\frac{2\pi k_e}{\omega Q}(T_{wb} - T_{ei})$$

$$T_D = -\frac{2I}{\pi}$$

2.9.2.Relaxation distance

When the temperature change of the formation due to medium transfer in a well is covered, the cooling of this mean must be discussed. Surroundings with a lower temperature cause the heat loss of a fluid. Ipek et al. (2002) stated, that fluid heat will be close to (or reach) equilibrium after some distance. Which corresponds to reaching an asymptote parallel to the geothermal gradient.

The relaxation distance (A_d) is introduced as a distance between the point of production (or inflow) and the point where flowing temperature gradient can be estimated by the geothermal gradient. Asymptote offset is controlled by several parameters like: flow rate, well geometry, well's time of production and fluid thermal properties.

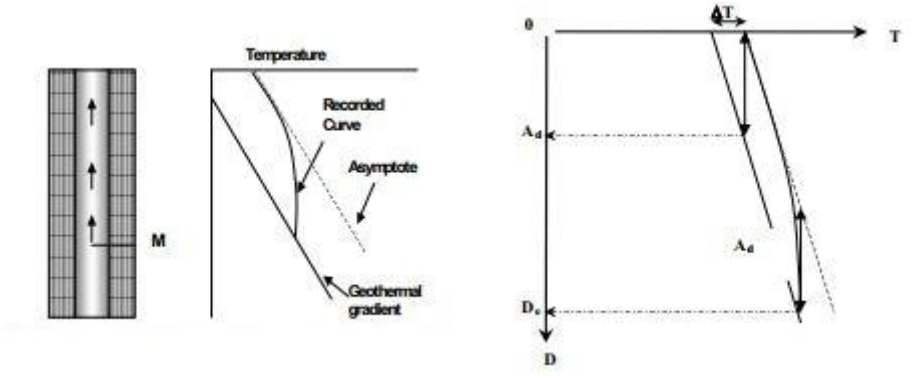

Figure 2-8. Temperature profile (left) and relaxation distance of a production well (right) (Ipek et al., 2002).

2.9.3.Nusselt number

Nusselt number is a dimensionless parameter characterizing convective heat transfer as a ratio of total to conductive heat transfer rate.

$$N_u = \frac{h2r}{k}$$

Where: h – conductive heat transfer coefficient

r – pipe wall inside radius at which the transfer takes place

k – thermal conductivity of the fluid

Depending on the mode, the Nusselt number can a function of various parameters, like: Reynold's, Prandtl or Grashof numbers. Bergman et al. (2011) pointed, that 'the Nusselt number is to the thermal boundary layer what the friction coefficient is to the velocity boundary layer'.

2.9.4.Reynolds

Reynold's number is one of the most important factor in fluid mechanics, predicting the flow behavior of the fluid. It is the ratio of inertial forces to viscous ones:

$$R_e = \frac{\rho v D}{\mu}$$

Where: ρ – fluid density

D – hydraulic diameter

μ – dynamic fluid viscosity

v – flow velocity

- laminar region of flow for Re ≤ 2300
- transitional region for 2300 < Re ≤ 4000
- turbulent region for Re > 4000

2.9.5.Prandtl number

Bergman et al. (2011) stated, that the Prandtl number is the ratio of momentum diffusion rate to thermal diffusion rate. It is given by the formula:

$$P_r = \frac{v}{\alpha} = \frac{\frac{\mu}{\rho}}{\frac{k}{c_p \rho}} = \frac{\mu c_p}{k}$$

Where: v – fluid momentum diffusivity

A – fluid thermal diffusivity

2.9.6.Grashof number

The Grashof number is a ratio of the buoyancy forces to the viscous forces in the velocity boundary layer. If two fluids have the same temperature, but the one which is more viscous, implying restricted movement, will have a smaller value of Grashof number. The parameter is given by:

$$G_r = \frac{g\beta(T_s - T_\infty)\rho^2 L^3}{\mu^2}$$

Where: β – thermal expansion coefficient

L – characteristic length

T_s – surface temperature

T∞– fluid temperature right outside the boundary layer

2.9.7.Rayleigh number

The Rayleigh parameter describes how the transfer of heat occurs throughout a fluid. It is connected to free (natural) convection. As mentioned before, fluid can only transport heat as conduction or convection in a presence of temperature gradient. Rayleigh number expresses which mode control the process of heat transfer.

$$R_a = G_r P_r$$

If Ra value is higher than the critical value, the transfer mode is a convection. When R_a is less than critical value the heat transfer happens through conduction (Bergman et al., 2011).

2.10.Governing equations for geothermal reservoir

Ganguly and Kumar (2012) identified, that geothermal reservoir simulation requires a proper mathematical model to achieve numerical solution that would describe the whole process. They stated five necessary requirements to obtain that:

- Physical and chemical processes operating in the reservoir,
- The initial conditions throughout the system and boundary conditions at the boundaries,
- Hydrogeologic parameters (porosity, permeability etc.) with their spatial variations,
- Fluid properties (density, viscosity, enthalpy vapor pressure etc.),
- The locations of sinks and sources and their flow rates.

As stated in point 2.3., single phase flow (water) is abnormal. Thus, the fluid flow is a complex phenomenon of several elements (usually water and steam, with dissolved CO_2 and NaCl), alternatively multiphase flow made from two phases water (liquid phase) and steam (gaseous phase) (Ganguly and Kumar, 2014). The core of numerical description lies on conservation equations or balance laws of mass momentum and energy. Characterization of the mathematical model was a subject of several researches, including Mercer et al. (1974), Faust and Mercer (1977), Brownell et al. (1977), Witherspoon et al. (1975). In all the above projects, authors pointed, that conservation equations should recognize each phase in the studied geothermal example. Then, the relations between them are applied to simplify and shorten the final answer. To make it possible, various sets of data can be used (temperature, enthalpy, pressure etc.).

Following partial differential equations govern the work of geothermal reservoir.

2.10.1.Mass energy balance

Mass conservation equations are usually introduced for two phases water wetting phase (w) and steam (s) non-wetting.

$$\frac{\partial(\emptyset S_s \rho_s)}{\partial t} + \nabla(\rho_s \overrightarrow{v_s}) - q_s - m = 0$$

$$\frac{\partial(\emptyset S_w \rho_w)}{\partial t} + \nabla(\rho_w \overrightarrow{v_w}) - q_w + m = 0$$

Where: ø – porosity

S – water saturation

ρ – density

q – source term

v – average phase flow velocity

m – mass transfer rate from liquid to vapor

2.10.2.Momentum balance

Momentum conservation equations are adapted from Newton's second law of dynamics and Darcy's Law for multiphase flow. In geothermal exploitation, the system consists of several fractures and the Darcy Law can be implemented as a dynamic or momentum formula.

$$\overrightarrow{v_s} = -\frac{K k_{rs}}{\mu_s}(\nabla p_s - \rho_s g \nabla D)$$

$$\overrightarrow{v_w} = -\frac{K k_{rw}}{\mu_w}(\nabla p_w - \rho_w g \nabla D)$$

Where: k_r – relative permeability

p – phase pressure

D – depth

K – intrinsic permeability tensor

g – gravitational constant

2.10.3.Energy balance

Energy balance formulas are the most extended part of preparing the model for geothermal exploration. They are primarily expressed in terms of pressure and enthalpy and the zero capillary pressure and local thermal equilibrium assumptions are needed.

$$\frac{\partial}{\partial t}[\emptyset\rho h' + (1-\emptyset)\rho_r h'_r] - \nabla\left[\frac{K k_{rs}\rho_s h'_s}{\mu_s}(\nabla p - \rho_s g \nabla D)\right] - \nabla\left[\frac{K k_{rw}\rho_w h'_w}{\mu_w}(\nabla p - \rho_w g \nabla D)\right] - \nabla[K_w(\frac{\partial T}{\partial p})_h \nabla p + K_w\left(\frac{\partial T}{\partial h}\right)_p \nabla h'\Big] - q_h = 0$$

Where: ρ – density of the total steam-water mixture

h'_w – enthalpy of water

h'_s – enthalpy of steam

h'_r – enthalpy of rock

h' – enthalpy of water steam mixture

T – temperature

q_h – source term

$$\rho = S_w\rho_w + S_s\rho_s$$

$$h' = \frac{S_s\rho_s h'_s + S_w\rho_w h'_w}{\rho}$$

And the individual phase saturations sum equal 1 (S_w+S_s=1).

According to Ganguly and Kumar (2012), simulating the geothermal exploitation is a complex multiphase flow problem. It consists of water in two states – liquid and steam. The complication of the governing formulas described above starts with dependence of capillary pressure and relative permeabilities of phases on saturation (p_c and k_r respectively). The relation between those parameters is called constitutive relationship. The capillary pressure is expressed as:

$$p_c = p_s - p_w$$

Where: p_s – non-wetting phase pressure of steam

p_w – wetting phase pressure of water

Commonly used terms of capillary pressure and saturation and relative permeability and saturation were introduced in by Brooks and Corey (1964):

$$p_c = p_d S_e^{\frac{1}{\lambda}}$$

$$k_{rw} = S_e^{\frac{2+3\lambda}{\lambda}}$$

$$k_{nw} = (1 - S_e)^2 \left(1 - S_e^{\frac{2+\lambda}{\lambda}}\right)$$

$$S_e = \frac{S_w - S_{rw}}{1 - S_{rw} - S_{rnw}}$$

Where: p_d – displacement pressure

λ – pore size distribution index

S_e – effective saturation of the wetting fluid

S_{rw} – residual saturation for wetting phase

S_{rnw} – residual saturation for non-wetting phase

k_{rw} – relative permeability for wetting phase

k_{nw} – relative permeability for non-wetting phase

O'Sullivan et al. (2001) stated that "a good understanding of the important aspects of the structure of the system and the most significant (physical and chemical) aspects in it is referred to as its conceptual model." It must consist of specific information about the formation, its temperature, geochemistry and reservoir's geothermal features.

When setting up the model for a geothermal exploitation, the boundary conditions must be chosen properly. At the base of the model the deep up-flow involves the large-scale convection of heat and mass by a suitable source.

2.11.Turbulence models

When the turbulence term is present in a particular flow, it dominates all over the other flow phenomena. A proper understanding of a certain turbulence model enables a successful numerical simulation to present the problem. The ideal example must comprise of geometry and grid set, exact physical model, solving and post-processing the computed data. The

challenge is project the complex phenomena with a simple model, so the idea is to minimize the complexity to show only the essence of physical state (Davidson, 2003).

The complexity of the turbulence model depends on the factors one wants to investigate in the simulation. The essence of Navier-Stokes equation is the core of the computation, but at the same time it has following features: nonlinearity, time-dependence and three-dimensional partial differential equations (Sodja, 2007).

In certain way, the turbulence is meant as the instable laminar flow that occurs at high Reynolds number. It comes from interactions between non-linear, inertial and viscous terms of Navier-Stokes equation. They are depended on time and rotational, as well as three-dimensional. Thus, there is no possibility to introduce the deterministic approach.

Hence, there are other methods to compute the turbulent flows. The main practice, which is introduced in the thesis, is the Reynolds-average Navier-Stokes equation (RANS). It requires less computational power than other methods and has following options (Sodja, 2007):

- eddy-viscosity models (EVM) – where it is assumed that the turbulent stress is proportional to the mean rate of strain. Thus, eddy viscosity is derived from turbulent transport equations (usually k + one other quantity),
- non-linear eddy-viscosity models (NLEVM) – here the turbulent stress is modelled as a non-linear function of mean velocity gradients. The scales are obtained by solving transport equations (as in EVM usually k + one other quantity). Case is analyzed to mimic response of turbulence to specific types of strain,
- differential stress models (DSM) – they comprised of Reynolds-stress transport models (RSTM) or second-order closure models (SOC). At least one is required to solve transport equations for all turbulent stresses.

Solving the fluid (in this case heat) transfer requires computational fluid dynamics (CFD) as this 3D problem needs 3D results with pressure and velocity fields. It is a crucial tool in a wide range of applications associated with fluid flow and heat transfer (Saha et al., 2011). In traditional drilling operations it is a main tool to formulate proper drilling cuttings transport scheme. The annular flow would not work with small velocities because the cuttings sedimentation at the bottom of the well needs to be avoided. On the other hand, too fast flows can harm the stability of the well (Neto et al., 2011). CFD investigations show that rotation of the pipe generates asymmetric distribution of cuttings along the well and considerably enhances the drag effects on working unit in tangential direction (Sun et al., 2014). Different approaches can be used varying if the case involves cuttings as a part of the problem (Eulerian-Eulerian concept) or as individual particles (Eulerian-Lagrangian) (Busch et al., 2016).

In general, the parameters controlled by the CFD may change with different approach used. To obtain detailed results of flow filed and velocity profiles, the computational fluid dynamics must be introduced (Bicalho et al., 2016). CFD completes experimental with theoretical work allowing building cases unavailable experimentally (Pereira et al., 2007).

In the following simulations, based on the work of Neto et al. (2011), five turbulence models were applied to investigate the most convenient case for the heat transfer.

2.11.1.Standard K-epsilon

One of the simplest models of practical engineering flow calculations. It is semi-empirical, based on two separate transport equations enabling turbulent velocity and length scales to be adjusted individually.

2.11.2.RNG K-epsilon

This model was developed to renormalize Navier-Stokes equations, so they could consider smaller scales of motion. It also has additional term to enhance the accuracy for rapidly strained flows so the whole system is more reliable for wider group of flows.

2.11.3.Standard K-omega

Another commonly recognized model with two transport equations representing turbulent properties of the flow. In this approach, there are two variables – specific dissipation (ω) regulating the scale of the turbulence and kinetic energy (k) governing the energy in the turbulence.

2.11.4.SST K-omega

Concept of combining robust and accurate management of the k-omega model in the region near the wall. It is comparable to standard k-omega approach but consists of a few new features – it covers a damped cross-diffusion derivative term in the 'ω' equation, the description of the turbulent viscosity is adjusted to consider transport of the turbulent shear stress. Moreover, the modeling constants are changed.

2.11.5.RSM

Reynolds stress model is a higher-level turbulence closure which serves as a most complete classical turbulence model. The eddy viscosity approach is neglected, so the individual elements of the Reynolds stress tensor are directly computed. RSM solves the transport equations for the Reynolds stresses, simultaneously with a formula for the dissipation rate. Thus, seven additional transport equations must be conducted in 3D. Since RSM considers several factors of streamline, rapid changes in strain rate etc., it has a strong potential to provide exact predictions for complex flows.

3. Simulation

3.1.Software

All the simulations were conducted using Ansys Workbench package from ANSYS Inc. The main tool to manage numerical simulations of flows is Fluent software. It is based on Reynolds Average Navier-Stokes (RANS) approach for turbulence models as it requires less computational cost than LES or DNS methodologies (Neto et al., 2014).

The CFD package is based on implementing numerical analysis to fluid flow and heat transfer to obtain approximate solutions of given issue. It is made from three core elements:

- Pre-processor (Space Claim or Design Modeler, Meshing) – creation of geometry and mesh,
- Solver (Fluent) – numerical solution of the fluid flow equations in computational domain,
- Post-processor (CFD-post) – analysis of the solution, results presentation in useful form.

The Ansys Fluent is established on Finite Volume Method (FVM) evaluating partial differential equations in the form of algebraic ones (LeVeque, 2002). Those values are estimated on at discrete places on meshed geometry. Term 'finite' indicates the small volume surrounding each node point of mesh. Ansys Workbench has a Graphical User Interface (GUI), so all the tools needed for simulations are presented on the main, single panel.

3.2.Solution methods

The SIMPLE algorithm for pressure velocity coupling was chosen. It stands for semi-implicit method for pressure-linked equations and uses the relationship between velocity and pressure corrections to carry out mass conservation and to obtain the pressure field.

Ansys Fluent was set on double precision mode with parallel processing option.

3.2.1.Spatial discretization

Several issues need to be determined before setting up the simulation. For instance, gradients are needed not only for establishing values of a scalar at the cell faces, but also for evaluating secondary diffusion terms and velocity derivatives. It was set for Least squares cell based, where the solution is assumed to change linearly.

PRESTO was chosen for pressure discretization scheme. It uses the discrete continuity balance for a 'staggered' control volume about the face to compute the 'staggered' (i.e. face) pressure (Patankar, 1980).

Second order upwind serves as a scheme for the momentum and energy evaluation as it is more accurate than the first one. At the same time first order upwind yields better convergence for 'cut cell' grid and rather simple flows thus it would be used for turbulent kinetic energy and dissipation rate.

3.2.2.Transient formulation

In general, every system or a process has a steady state when all the variables are consistent in time. It has an easier convergence because there are fewer terms to analyze and some of the non-linearities are neglected. One of the purposes of this study is to show the behavior of the medium in certain period. Therefore, for all the cases the transient calculation was conducted. In order to do that, transient formulation method was set on second order implicit- the accuracy was improved with the implicit formation of pressure-based solver.

3.3.Cases

Two different sets of dimensions for the pipes were analyzed. First series (referred as 'small dimensions') was taken from research conducted by Neto et al. (2011) and after adapting five turbulence models on it, the most convenient one was applied on dimensions normally used on the field (referred as 'true dimensions'). Larger parameters are usually connected to the investors' expectations of increased flow rate (Serpen & Başel, 2015). For both sizes the concentric and eccentric options were investigated. The eccentricity of the inner pipe is a very common issue in drilling or production processes. It should be addressed in every operation in wellbore to fully understand the possible effects.

3.3.1.Small dimensions

Parameter	Symbol	Value [inch]	Value [mm]
Outer diameter	D_o	1,588	40,3
Outer radius	R_o	0,794	20,15
Inner diameter	D_i	0,788	20
Inner radius	R_i	0,394	10
Hydraulic diameter	D_h	0,799	20,3
Computational length	L_z	3,979	101
Eccentricity	e	0,5[-]	0,5 [-]
Distance between centers of inner and outer pipe	L	0,2	5,08

Table 3-1. Dimensions of first case.

The computational length of the pipe was calculated based on the following equation:

$$L_z = 5 * D_h$$

The eccentricity of the pipes was chosen for the value of 0,5 based on publications from Nouri et al. (1993) and Nouri & Whitelaw (1997).

$$e = \frac{L}{R_o - R_i}$$

$$L = e(R_o - R_i)$$

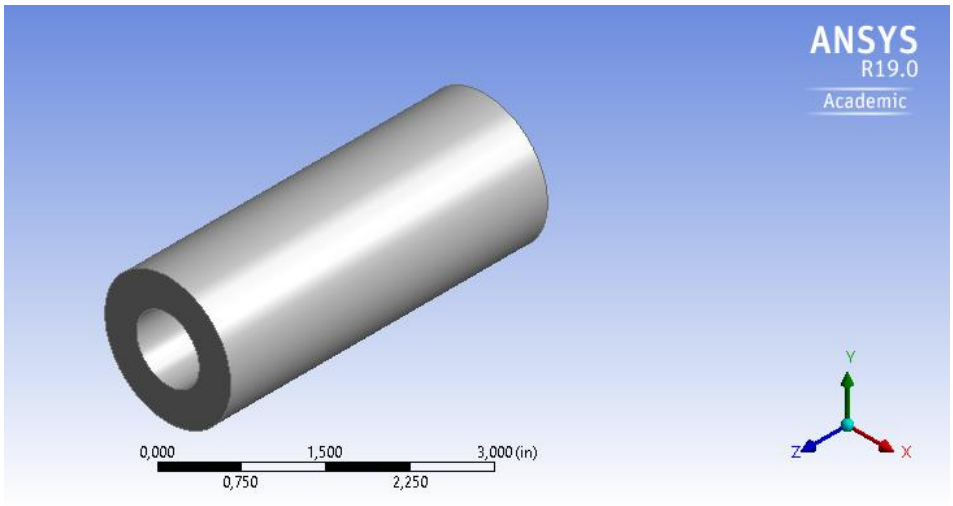

Figure 3-1. Small dimensions' concentric pipe. Image from Design Modeler.

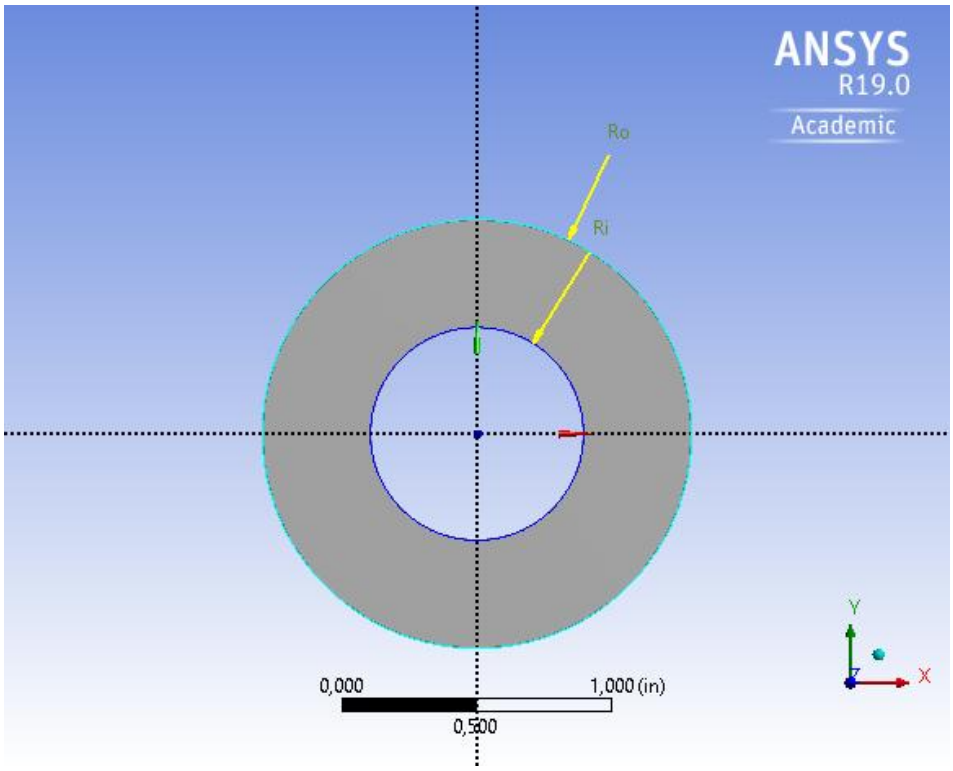

Figure 3-2. Front view of concentric pipe.

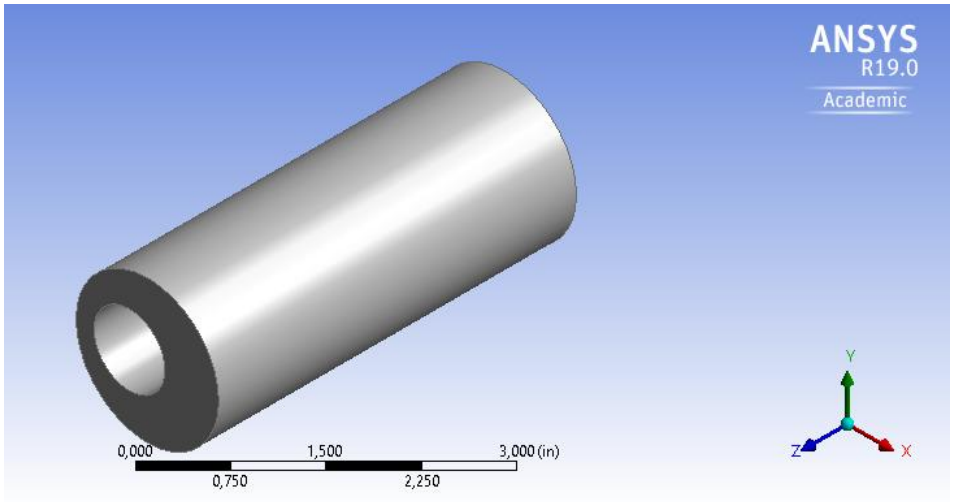

Figure 3-3. Small dimensions' eccentric pipe.

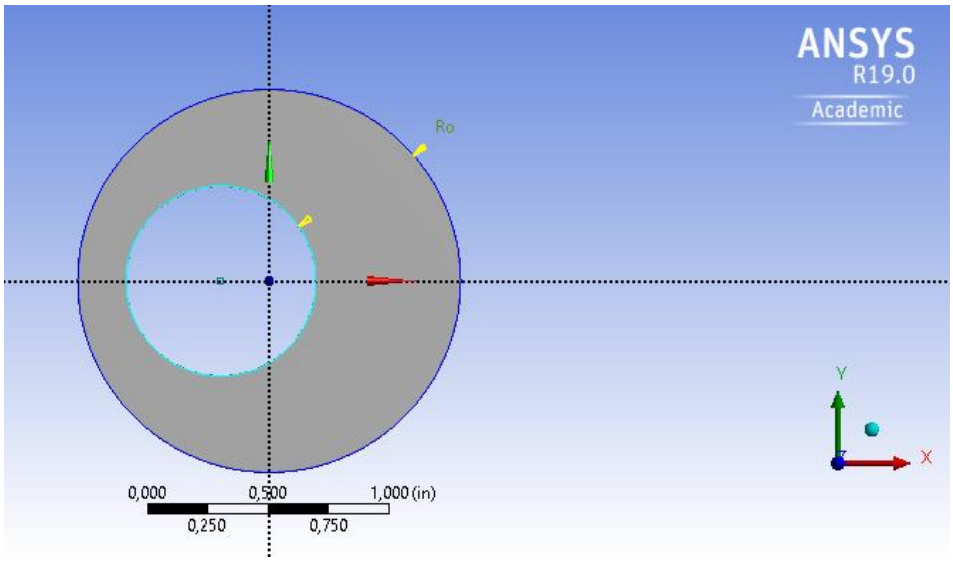

Figure 3-4. Front view of eccentric pipe.

3.3.2.True dimensions

Parameter	Symbol	Value [inch]	Value [mm]
Outer diameter	D_o	7	177,8
Outer radius	R_o	3,5	88,9
Inner diameter	D_i	4,5	114,3
Inner radius	R_i	2,25	57,15
Hydraulic diameter	D_h	2,5	63,5
Computational length	L_z	12,5	317,5
Eccentricity	e	0,5[-]	0,5 [-]
Distance between centers of inner and outer pipe	L	0,625	15,88

Table 3-2. Dimensions of second case.

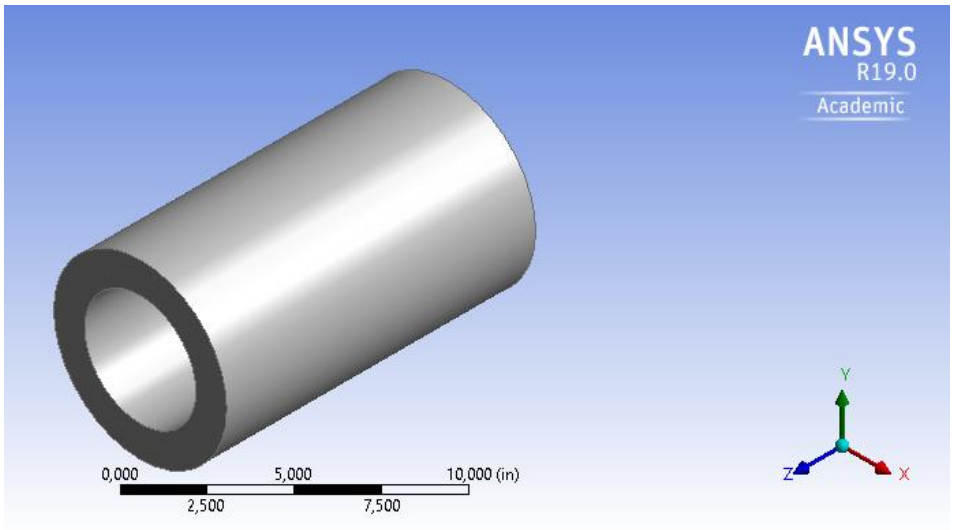

Figure 3-5. True dimensions' concentric pipe.

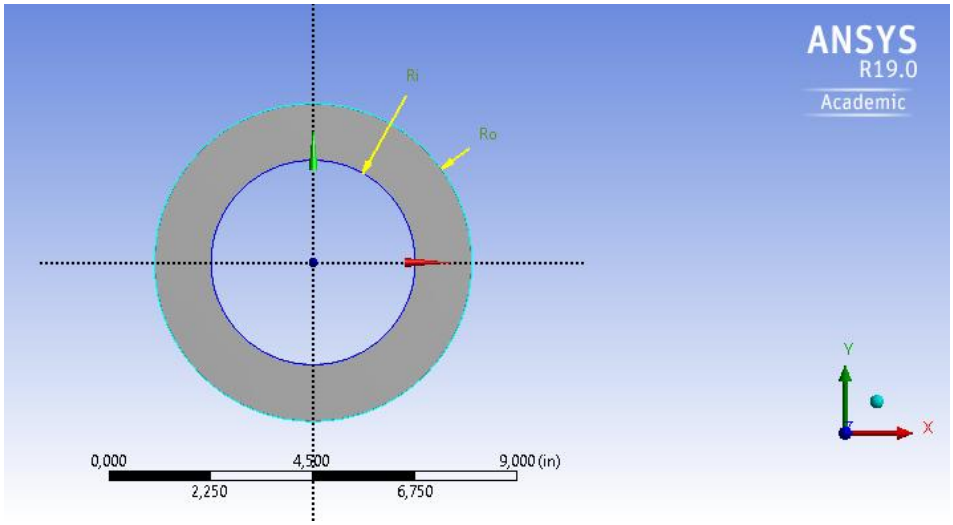

Figure 3-6. Front view of concentric pipe.

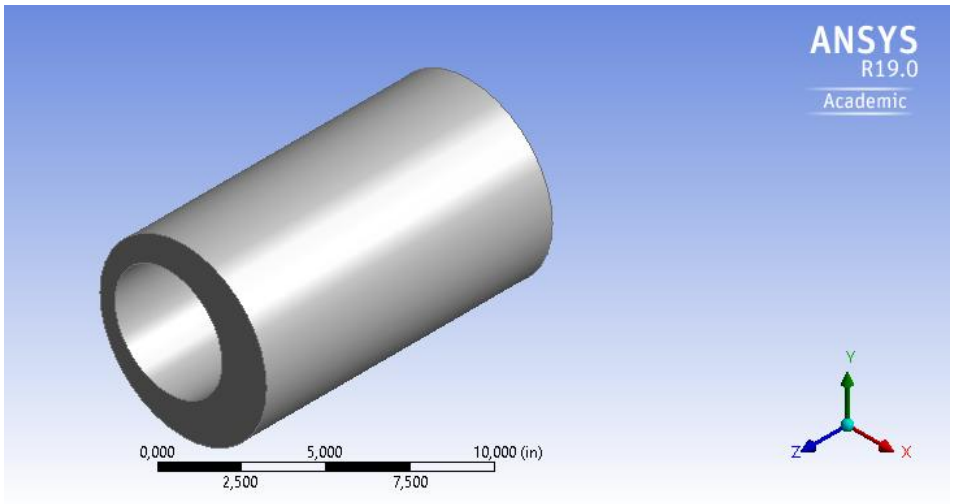

Figure 3-7. True dimensions' eccentric pipe.

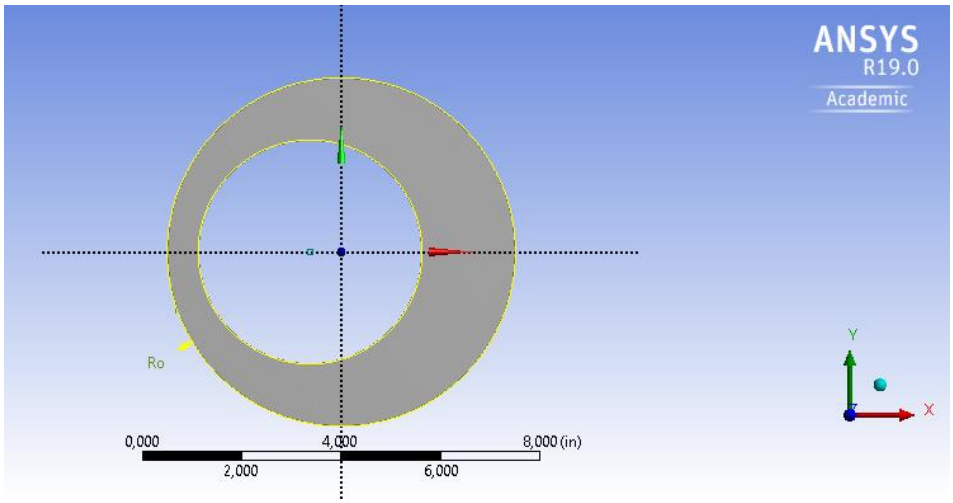

Figure 3-8. Front view of eccentric pipe.

3.4.Meshing

Meshing was obtained within the Ansys package.

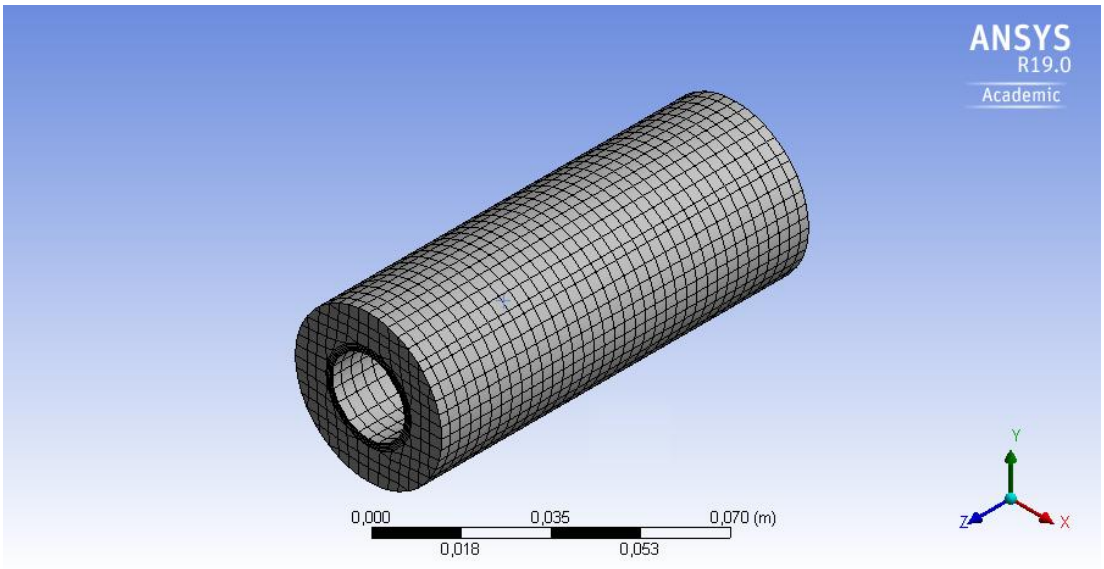

Figure 3-9. Meshing of the concentric 'small dimensions' case.

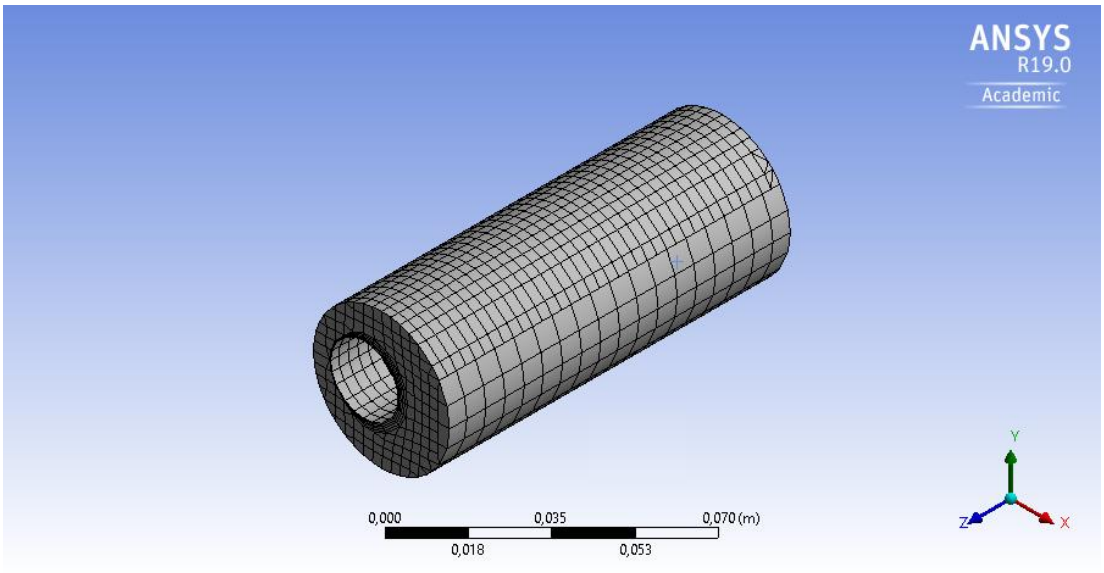

Figure 3-10. Meshing of the eccentric 'small dimensions' case.

Case	Number of nodes	Number of elements
Small dimensions concentric	9472	8496
Small dimensions eccentric	9200	8292
True dimensions concentric	2516	2176
True dimensions eccentric	4420	3972

Table 3-3. Meshing statistics.

3.5.Input data

Most of the input data was taken from the project conducted by Neto et al. (2011) and the working fluid for the simulations was chosen to be water, as it expresses the standard case of geothermal exploitation. All simulations were conducted with gravity factor for more realistic scheme.

Parameter	Value	Unit
Velocity	2,14	m/s
Temperature	25	^{o}C
Density	1	kg/m^3
Specific heat	4216	J/kgK
Thermal conductivity	0,677	w/mK
Viscosity	0,0008	kg/ms
Gravity	9,81	m/s^2

Table 3-4. Parameters of working fluid.

Parameter	Type of boundary condition
Inlet	Velocity-inlet
Outlet	Outflow
External pipe	Symmetry
Internal pipe	Wall
Annulus	interior

Table 3-5. Boundary conditions from Ansys Fluent for domains.

In the 'wall' boundary condition, the shear status was set to 'no-slip'. The interface of the annulus and outer pipe is fluid-solid, which means that fluid particles in contact with solid wall are attached to the solid particles.

Parameter	Value	Unit
Density	2719	kg/m^3
Specific heat	871	J/kg-K
Thermal conductivity	202,4	W/m-K

Table 3-6. Parameters of material set for 'wall' boundary condition (inner pipe).

Parameter	Value
Max iterations/time step	50
Time step size	0,01
Number of time steps	200
Convergence	0,0001

Table 3-7. Solution parameters for transient formulation.

4. Results and discussions

4.1.Concentric assembly of small dimensions

4.1.1.Residuals

Residuals are the error magnitudes for equations as iterations continue. Those equations involve momentum equations, continuity (conservation of mass) and energy calculations. The residual is the difference between the former and present result of iteration. If those errors are declining, the solution is converging- results have values that are changing less and less. The convergence was set before with a value of 0,0001.

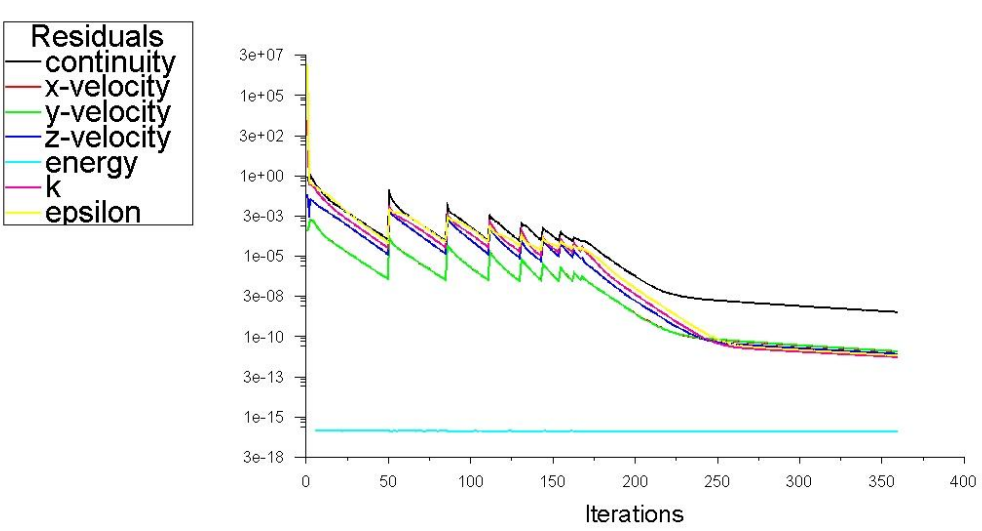

Figure 4-1. Residuals for concentric standard K-e model.

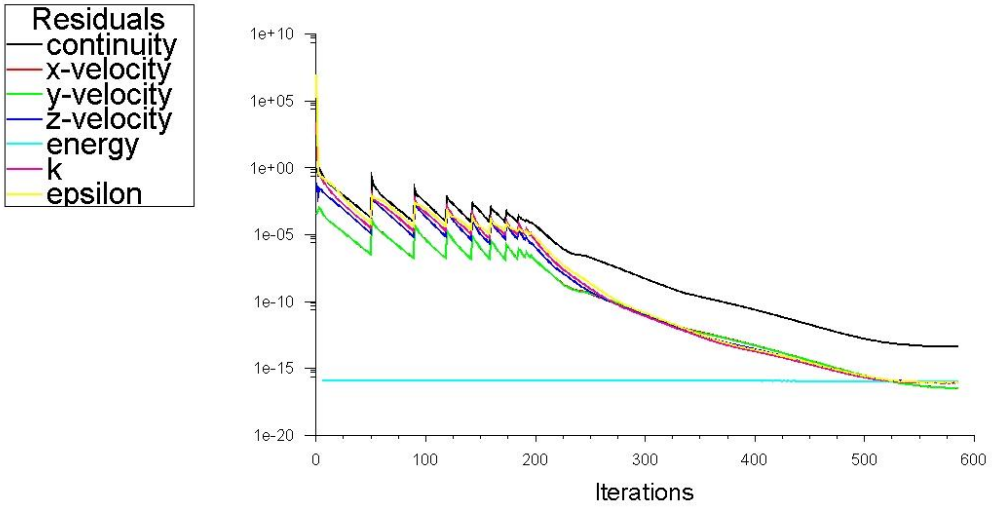

Figure 4-2. Residuals for concentric RNG K-e model.

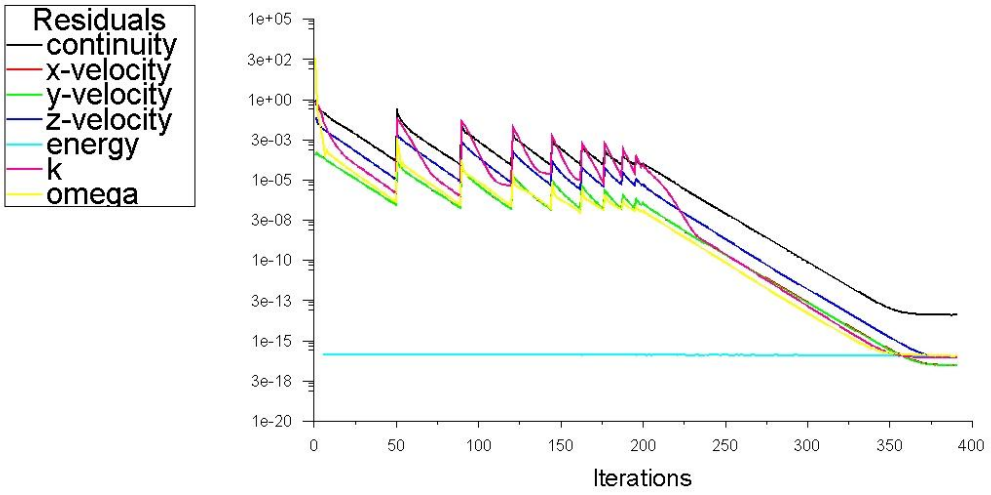

Figure 4-3. Residuals for concentric standard K-w model.

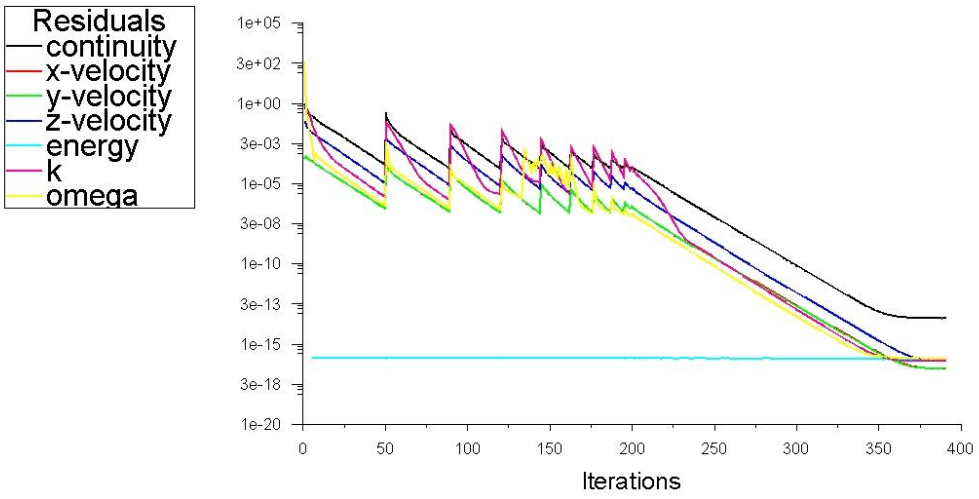

Figure 4-4. Residuals for concentric SST K-w model.

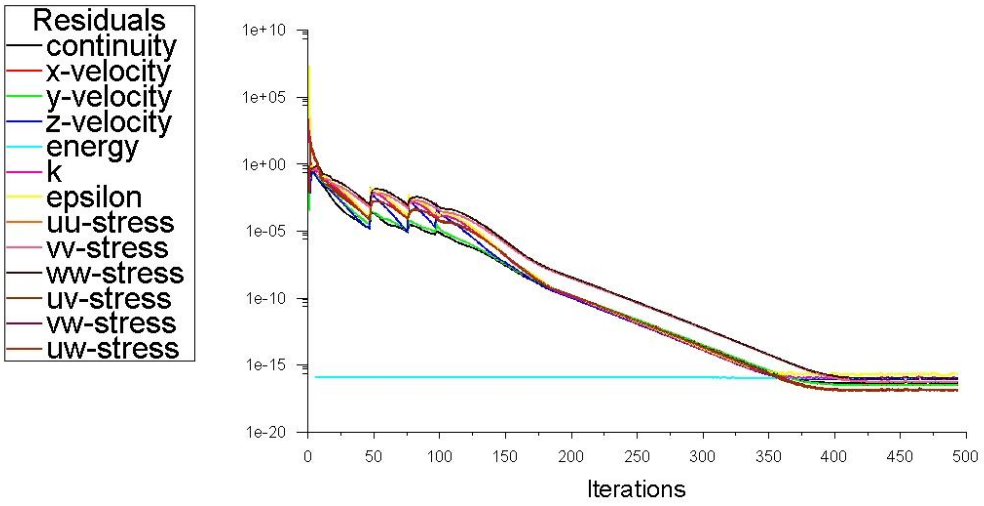

Figure 4-5. Residuals for concentric RSM model.

As it can be seen above, the standard K-epsilon model (Figure 4-1.) finished the simulation first, after around 350 iterations. The last model to do so, was the RNG K-epsilon (Figure 4-2.). Despite that, all the parameters in first four turbulence model seem to differ in a way. Only in the RSM model they are aligned more precisely. Moreover, as the transient state was applied, all the models are moving towards steady state. In all the cases energy parameters remain constant.

4.1.2.Streamlines and vortex regions

Vortex is a region in a fluid in which the flow rotates around the axis line. Vortex region is described as a special type of isosurface. The streamlines, as the paths of particles of zero mass through fluid, are actually affected by the vortex structure. It can be observed that streamlines are only interrupted near 'wall' as a boundary condition (inner pipe) and not near the outer pipe, as it is set as 'symmetry' boundary. The below projections were made after the end of simulation to show the final distribution of particular parameters.

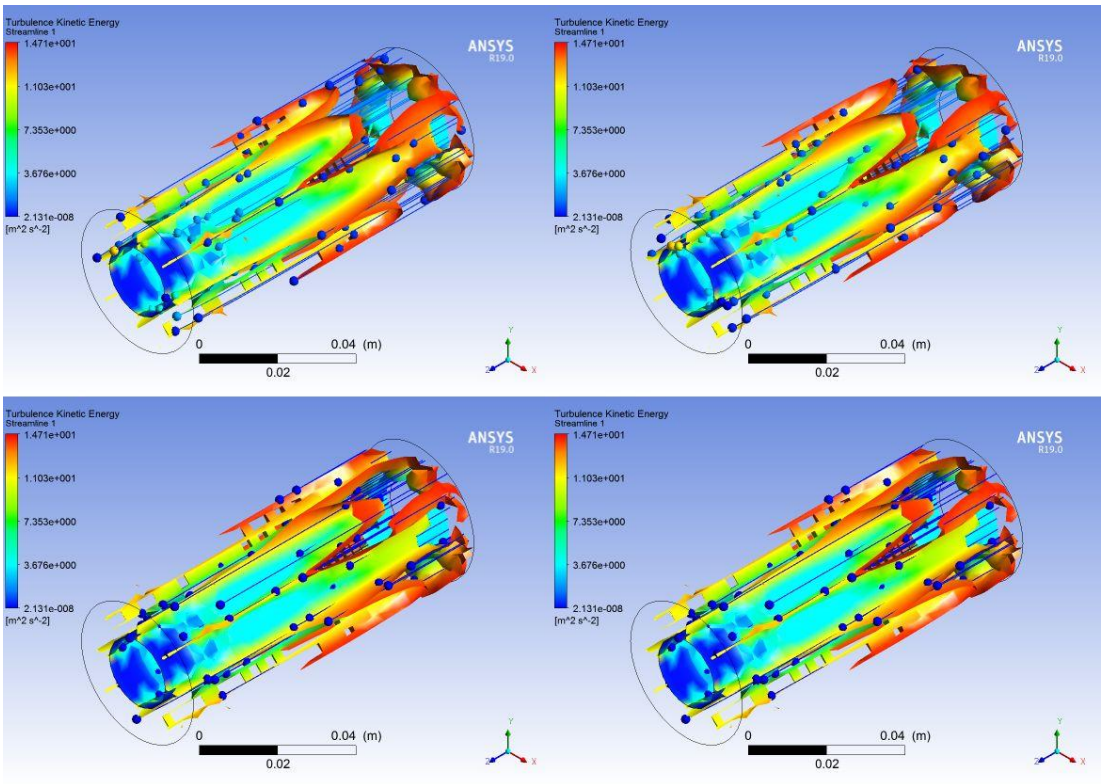

Figure 4-6. Streamlines and vortex regions for concentric standard K-e, RNG K-e, standard K-w, SST K-w models.

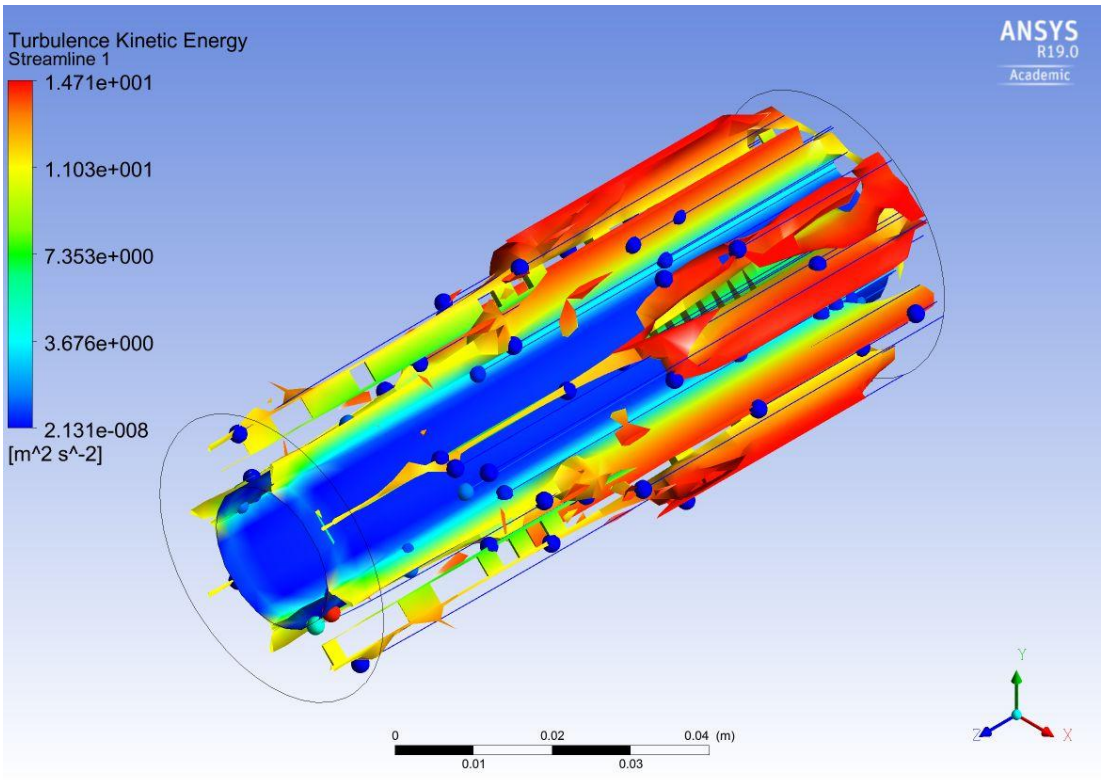

Figure 4-7. Streamlines and vortex region for concentric RSM model.

Vortex cores for main turbulence models are generally very similar to each other despite the additional equations (Figure 4-8.). Standard K-epsilon example has slightly smaller vortex near the outer pipe than RNG K-epsilon pattern in the same location. For K-omega standard and SST approaches, the results are nearly the same for given input parameters. The only model with diverse outcome is the RSM (Figure 4-7.), it has higher values of TKE (Turbulence Kinetic Energy) (as the mean kinetic energy per unit mass associated with eddies in turbulent flow) near the outer pipe. TKE is the energy content of eddies in turbulent flows. Bigger sizes correspond to higher energy content of eddies. This parameter is extracted from the mean flow of larger eddies, from larger eddies to smaller ones and eventually dissipates in considerably small eddies where viscous effects overpower the kinetic energy.

4.1.3.Vectors of pressures

Constant pressure was applied in every investigated model. As can be observed in the Figure 4-8., on the 'symmetry' boundary condition it has nearly the same distribution for first four models, with slightly higher values for K-epsilon approaches, both standard and RNG, at the velocity inlet. Along the given element pressure decreases regularly. For the RSM model (Figure 4-9.) pressure behaves in the exact same way along the pipe but starts with a higher value. Both figures represent the pressure distribution after the determined simulation time of 2 seconds.

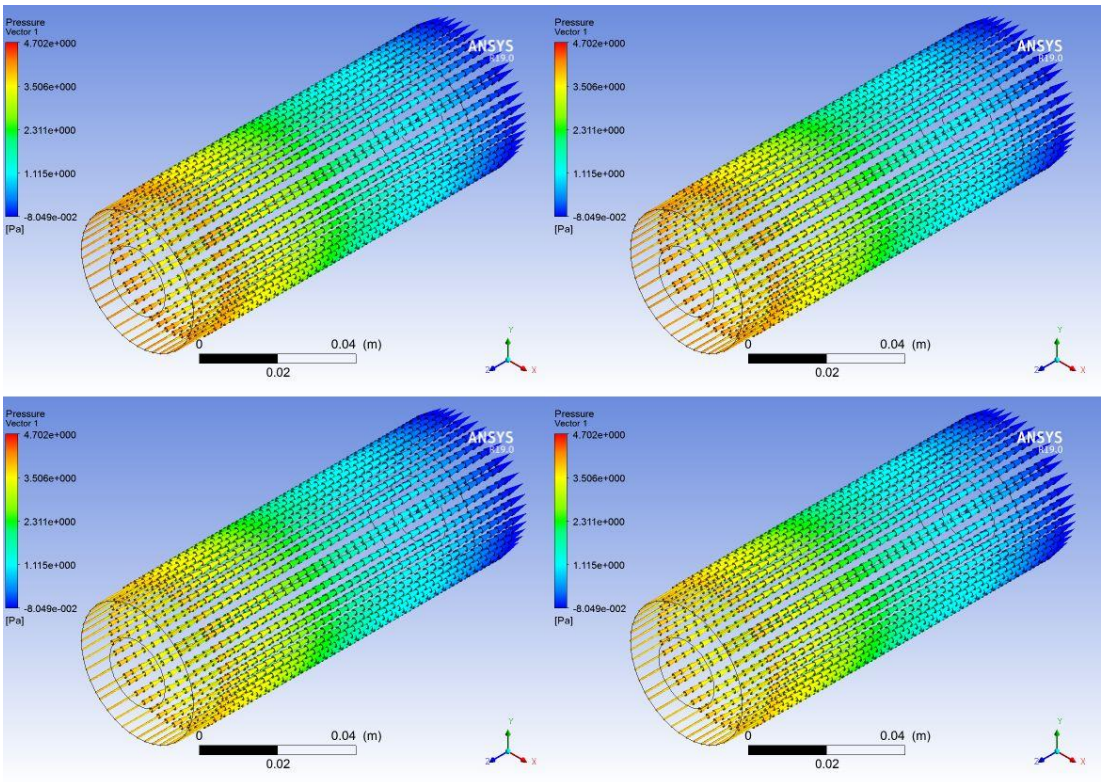

Figure 4-8. Vectors of pressures for concentric standard K-e, RNG K-e, standard K-w, SST K-w models.

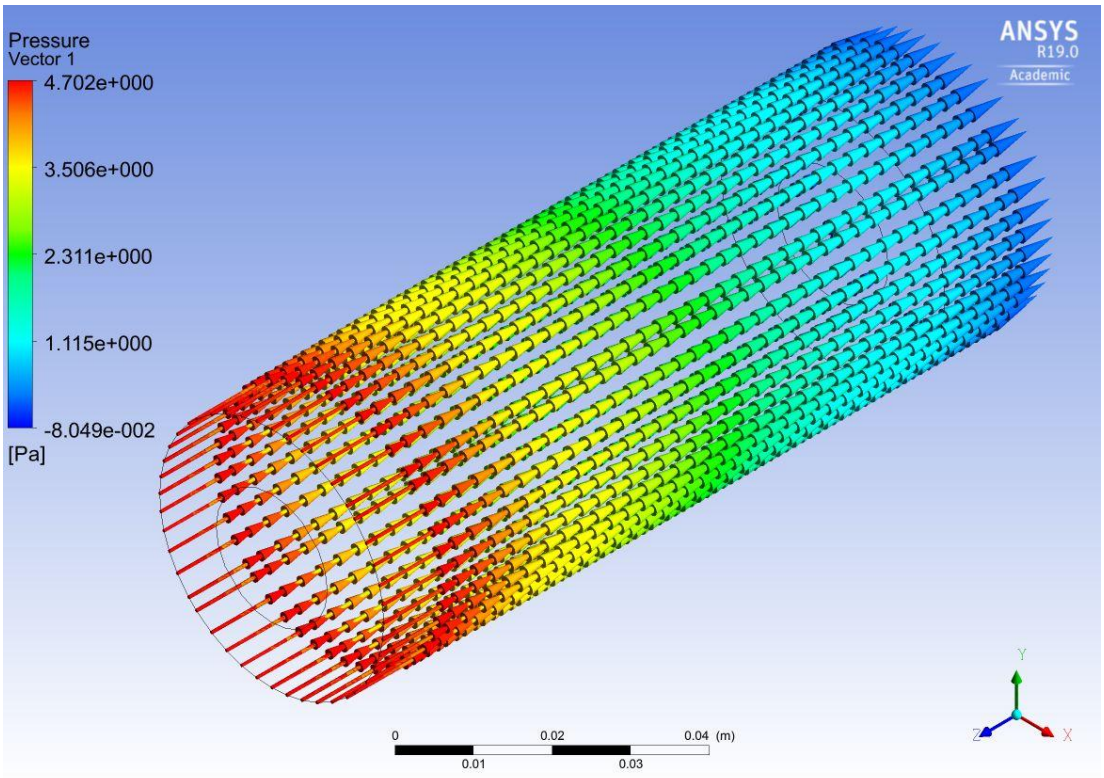

Figure 4-9. Vectors of pressure for concentric RSM model.

4.1.4.Contours of velocity

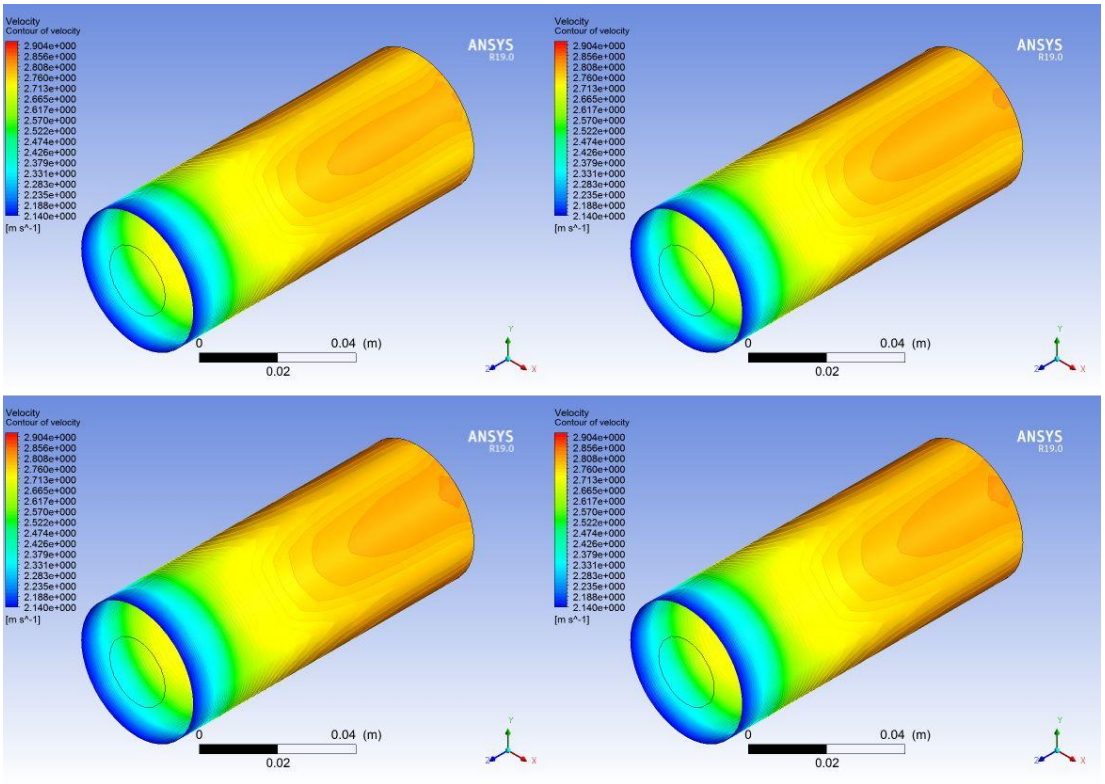

Figure 4-10. Contours of velocity for concentric standard K-e, RNG K-e, standard K-w, SST K-w models.

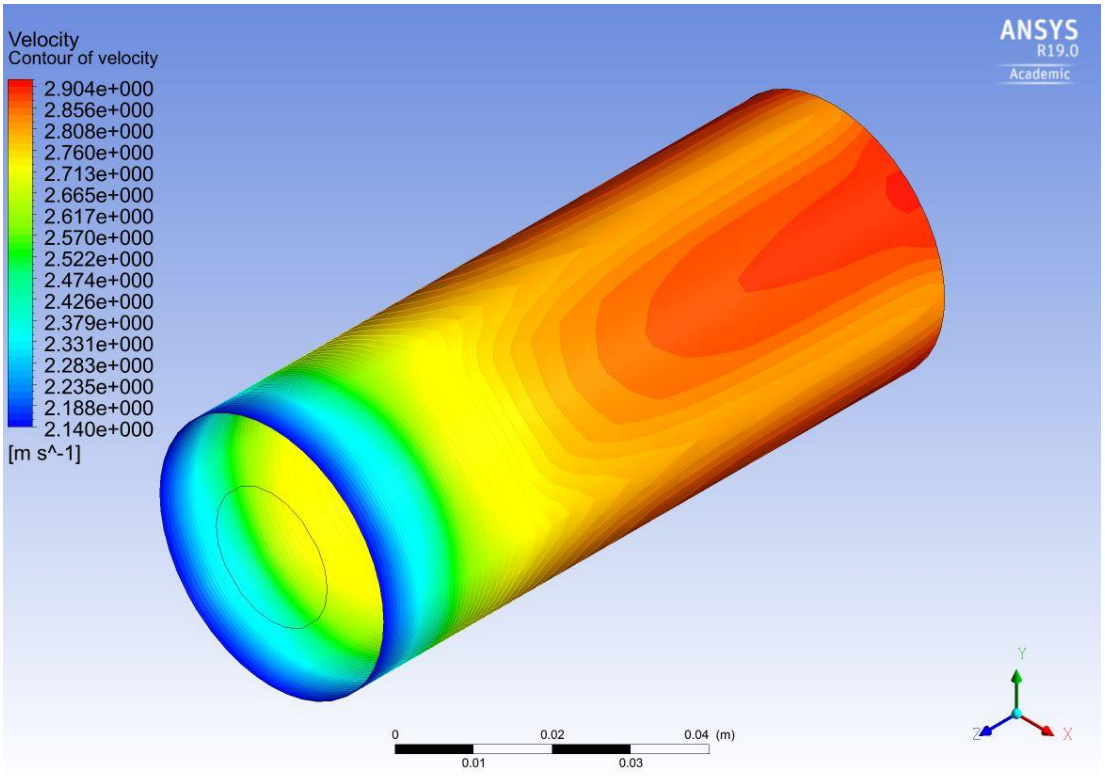

Figure 4-11. Contours of velocity for concentric RSM model.

Preceding contours of velocity represent the situation after completing the simulation (after 2 seconds). In each case the velocity over the symmetry (outer pipe) increases with the flow. Alike the previous parameters, velocity for standard and RNG K-epsilon models and standard and SST K-omega (Figure 4-10.) are very much comparable. The RSM option gives higher values of velocity in the same positions.

4.1.5.Velocity along the annulus

Allocation of velocity changes with the distance from the inner pipe. Values increase from this position reach the highest values at the symmetry (outer pipe) as shown before. To investigate the behavior of velocity for turbulence models inside the annulus, the following chart was created representing changes along the line located in the middle of the annulus.

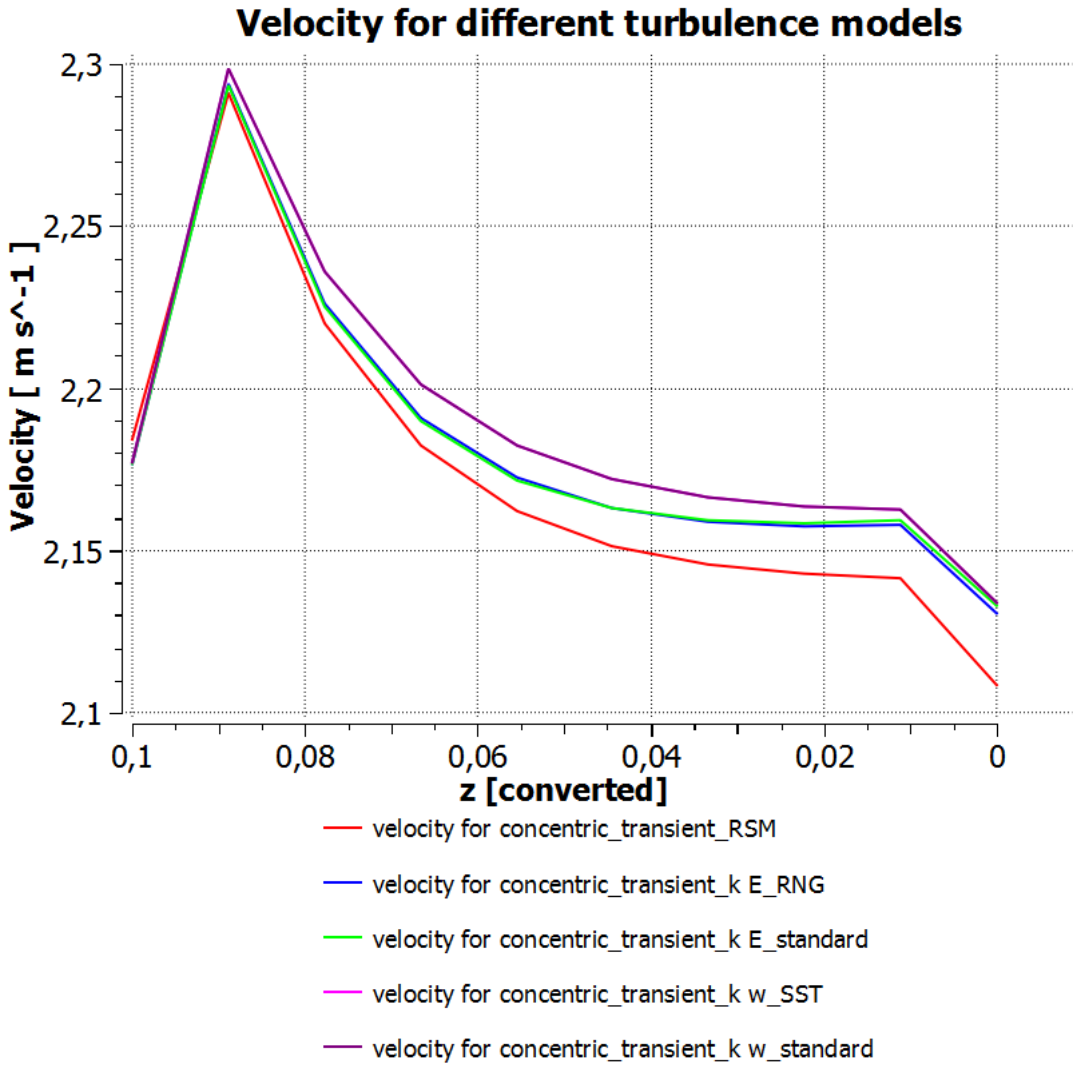

Figure 4-12. Velocity values along the annulus for concentric assembly for different turbulence models.

The ‘z’ factor stands for the distance from the velocity inlet towards the outflow. As the boundary condition of those elements were set inversely to ‘z’ axis in cartesian coordinate system, in the chart it must have been converted to show the true situation. It should be analyzed as the distance towards the point (0,0,0) in the system, corresponding to outflow. From the inlet velocities follow the same path, they increase intensely to hit their highest values, after which they decrease hyperbolically to certain point and at the end they drop linearly. In this situation the RSM model obtains lowest values and the standard and RNG K-epsilon deliver better results.

4.2.Selection of preferred model for concentric assembly with true dimensions

For most of the cases Reynolds stress model gives better results, which, as mentioned before, is a higher-level turbulence closure that serves as a most complete classical turbulence model. At the same time, it better fits complex flows or movement in rather complicated elements. This simulation is based on simple scenarios both for geometry and physical input parameters, so there is no need to adjust such advanced methods of numerical simulation. Thus, preferred method of investigation the flow in the annulus established on ‘true dimensions’ (determined before) would be simpler standard K-epsilon. Values of heat transfer rate obtained from the ‘Flux Report’ in Ansys also indicates this model for a most convenient one in this scenario.

4.3.Eccentric assembly of small dimensions

4.3.1. Residuals

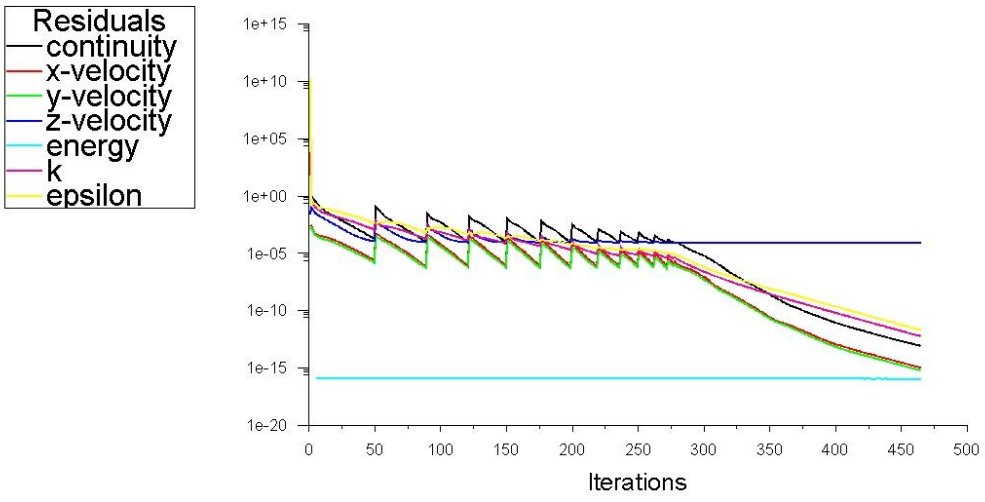

Figure 4-13. Residuals for eccentric standard K-e model.

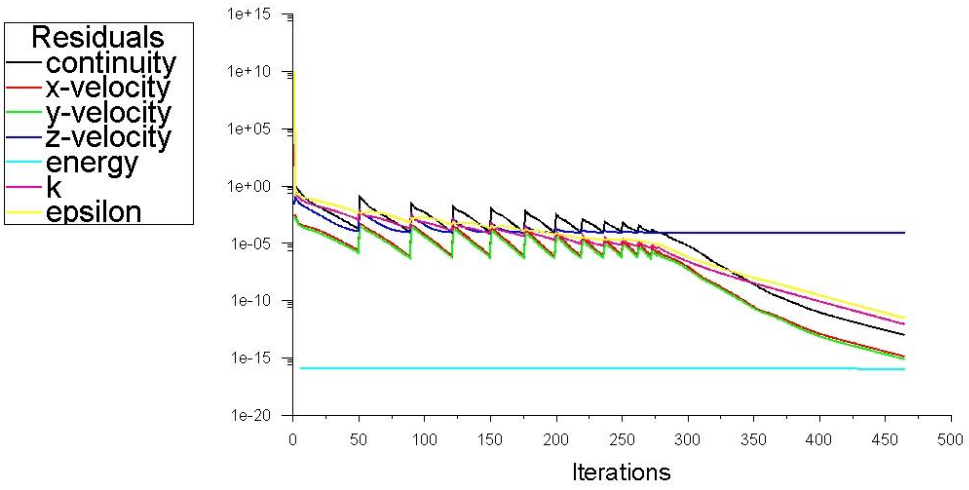

Figure 4-14. Residuals for eccentric RNG K-e model.

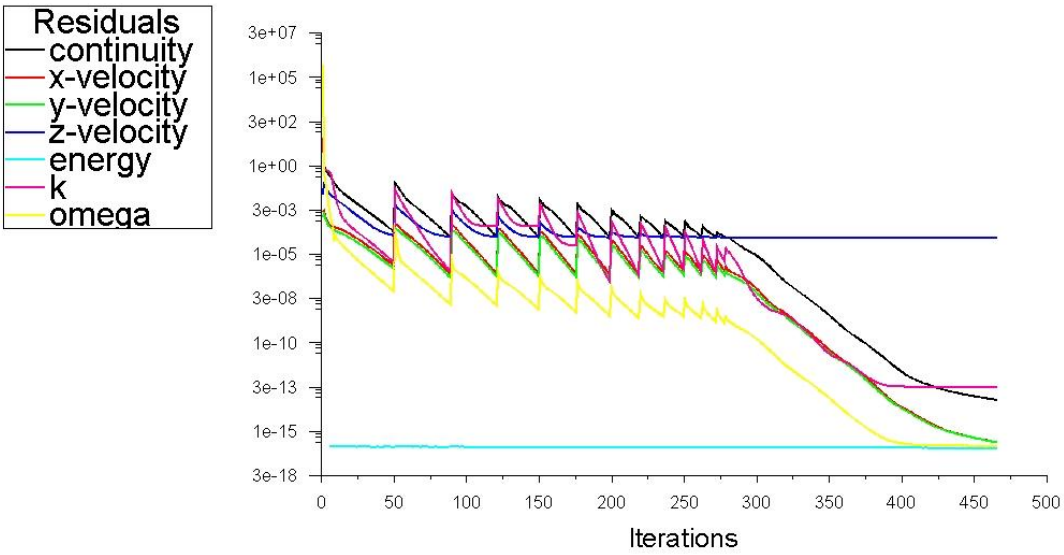

Figure 4-15. Residuals for eccentric standard K-w model.

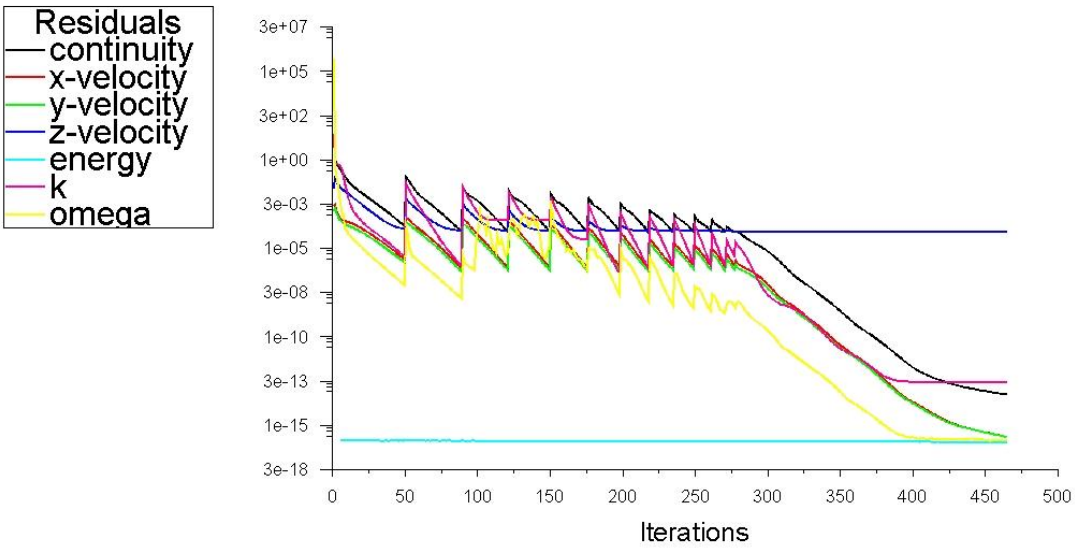

Figure 4-16. Residuals for eccentric SST K-w model.

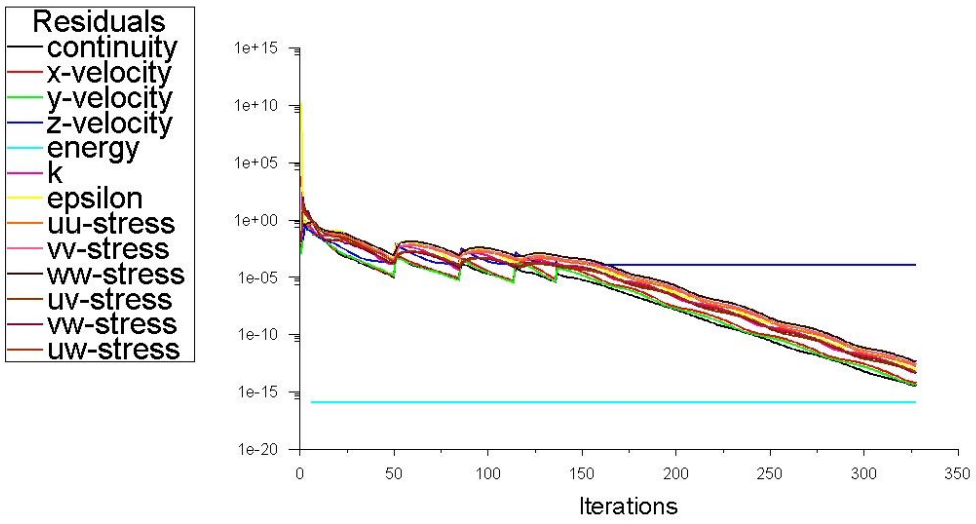

Figure 4-17. Residuals for eccentric RSM-w model.

While all the turbulence models for eccentric assembly obtained the determined convergence, first four of them (standard K-e, RNG K-e, standard K-w, SST K-w) have major diversities in particular residuals rates. Only Reynolds stress model shows better arrangement of those factors. Nonetheless, the z-velocity (determined input parameter) do not merge with other elements, which implies that models do not meet the steady state. One of the reasons for that situation might be the asymmetry of the investigated element or the improper meshing technique. In all the cases energy parameters remain constant.

4.3.2.Streamlines and vortex regions

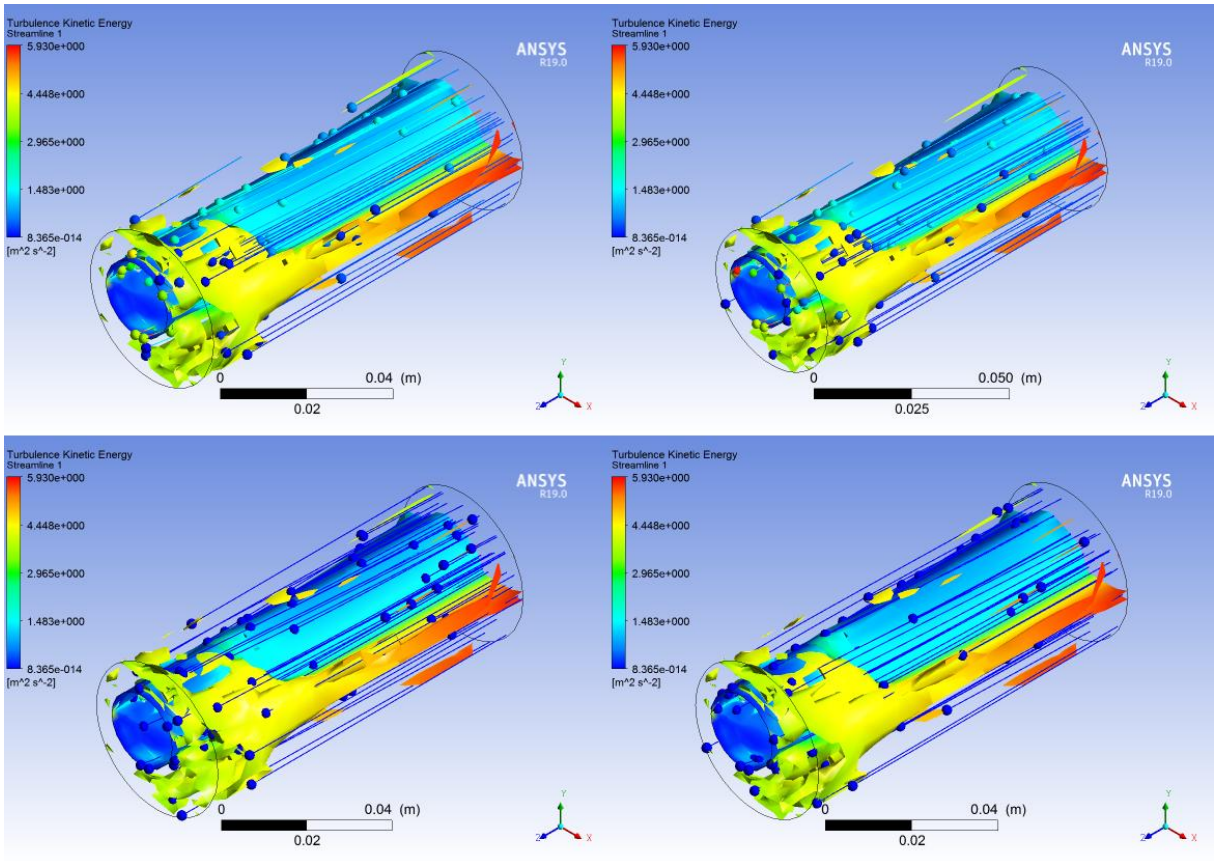

Figure 4-18. Streamlines and vortex regions for eccentric standard K-e, RNG K-e, standard K-w, SST K-w models.

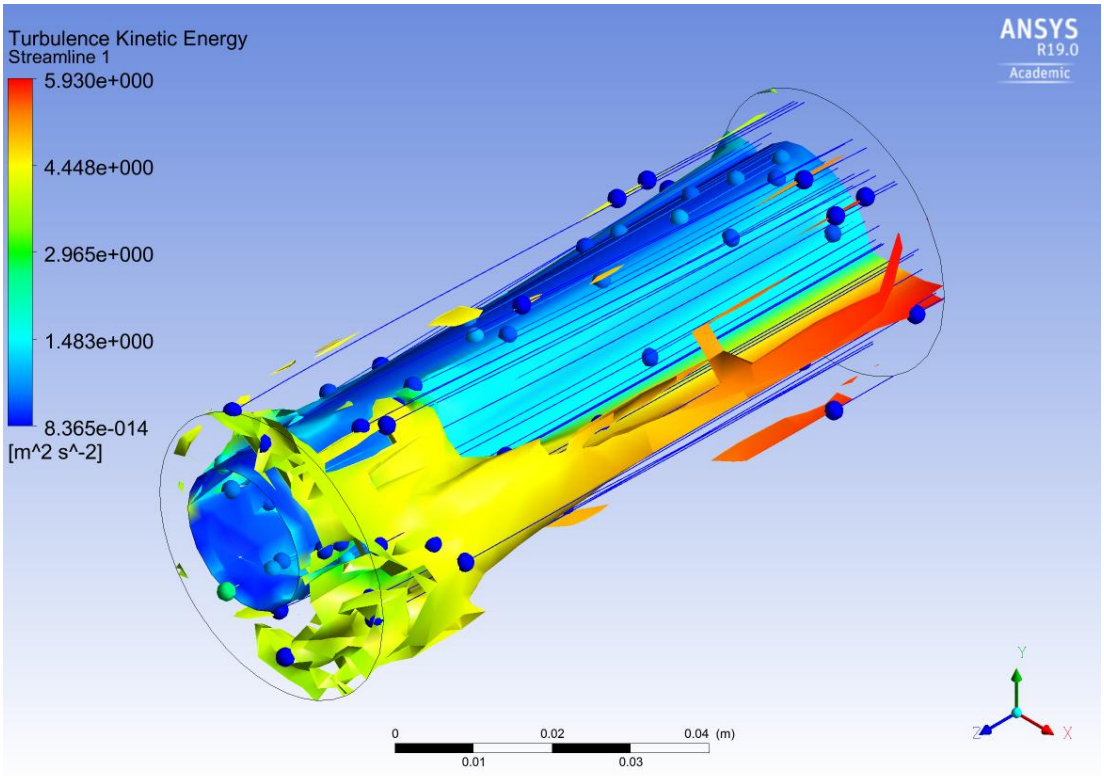

Figure 4-19. Streamlines and vortex region for eccentric RSM model.

The streamlines and vortex regions show high resemblance. Unlike the previous assembly of small dimensions, here all the models follow similar path. At the end of the simulation the vortex region around the velocity inlet suggest larger movement, but with relatively small values of TKE. Greater results are obtained in the large gap in the annulus at the end of the pipes. In the narrow gap there is almost no sign of those structures.

4.3.3.Vectors of pressures

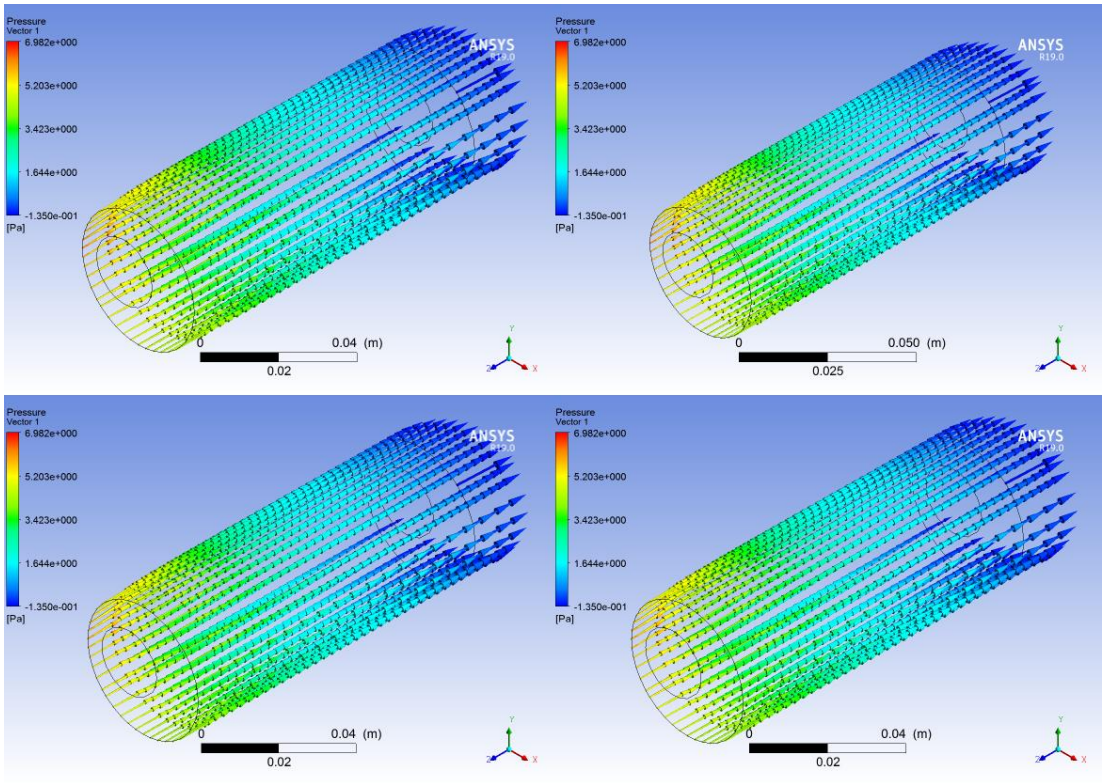

Figure 4-20. Vectors of pressures for eccentric standard K-e, RNG K-e, standard K-w, SST K-w models.

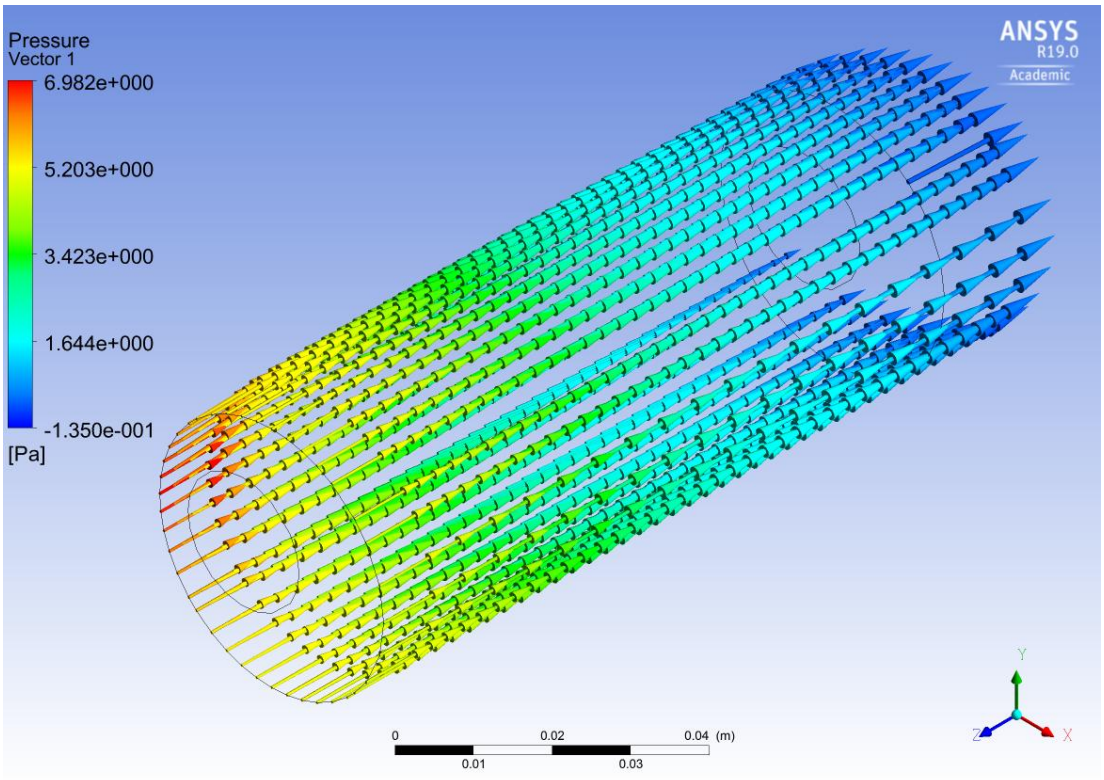

Figure 4-21. Vectors of pressure for eccentric RSM model.

Vectors of pressure on the 'symmetry' (outer pipe) have clearly higher values near the narrow gap of the annulus than in the larger gap. The distribution of pressure in the annulus of eccentric assembly in general is comparable to the concentric arrangement, which means the decrease of pressure values along the outer pipe with the flow direction.

4.3.4.Contours of velocity

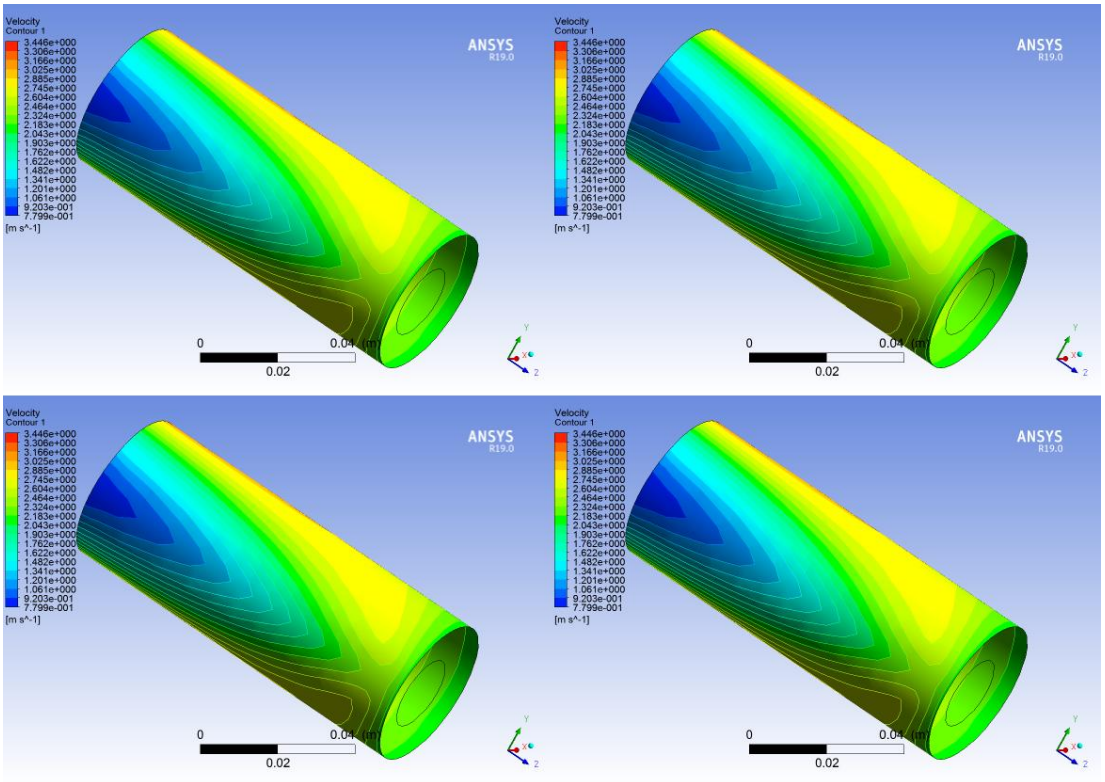

Figure 4-22. Contours of velocity for eccentric standard K-e, RNG K-e, standard K-w, SST K-w models.

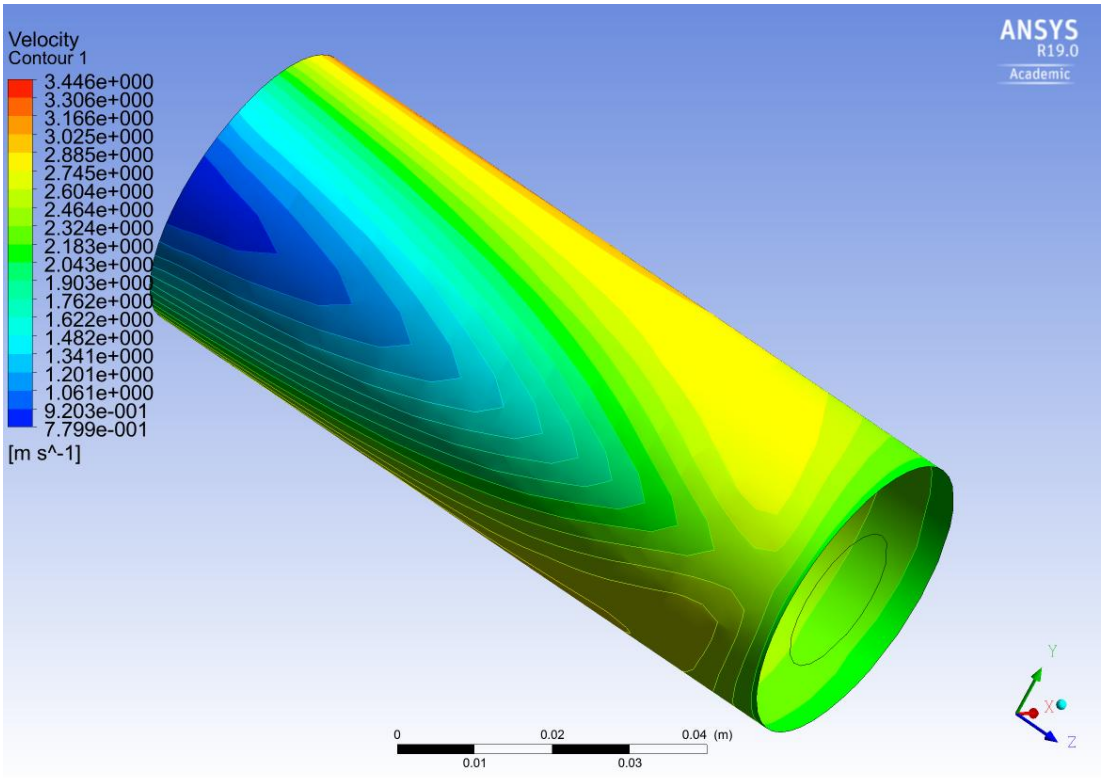

Figure 4-23. Contours of velocity for eccentric RSM model.

As for the contours of velocity, in all analyzed models the lowest results are on the 'symmetry' boundary over the narrow gap of the annulus. Values decrease along the pipe length in this region. At the same time on the other side of the assembly, over the larger gap, the values are a little bit higher.

4.3.5.Velocity along the annulus

Distribution of the velocity along the distance from the inlet towards the outlet was shown on the following charts. The first one (Figure 4-24.) represents the changes in the middle of the larger gap in the annulus and the second one (Figure 4-25.) states the situation in the middle of the narrow gap. Same, as in the concentric cases, the 'z' factor stands for the distance from the velocity inlet towards the outflow and it is inversed to serve the true investigation of velocity change from the velocity inlet towards the outflow.

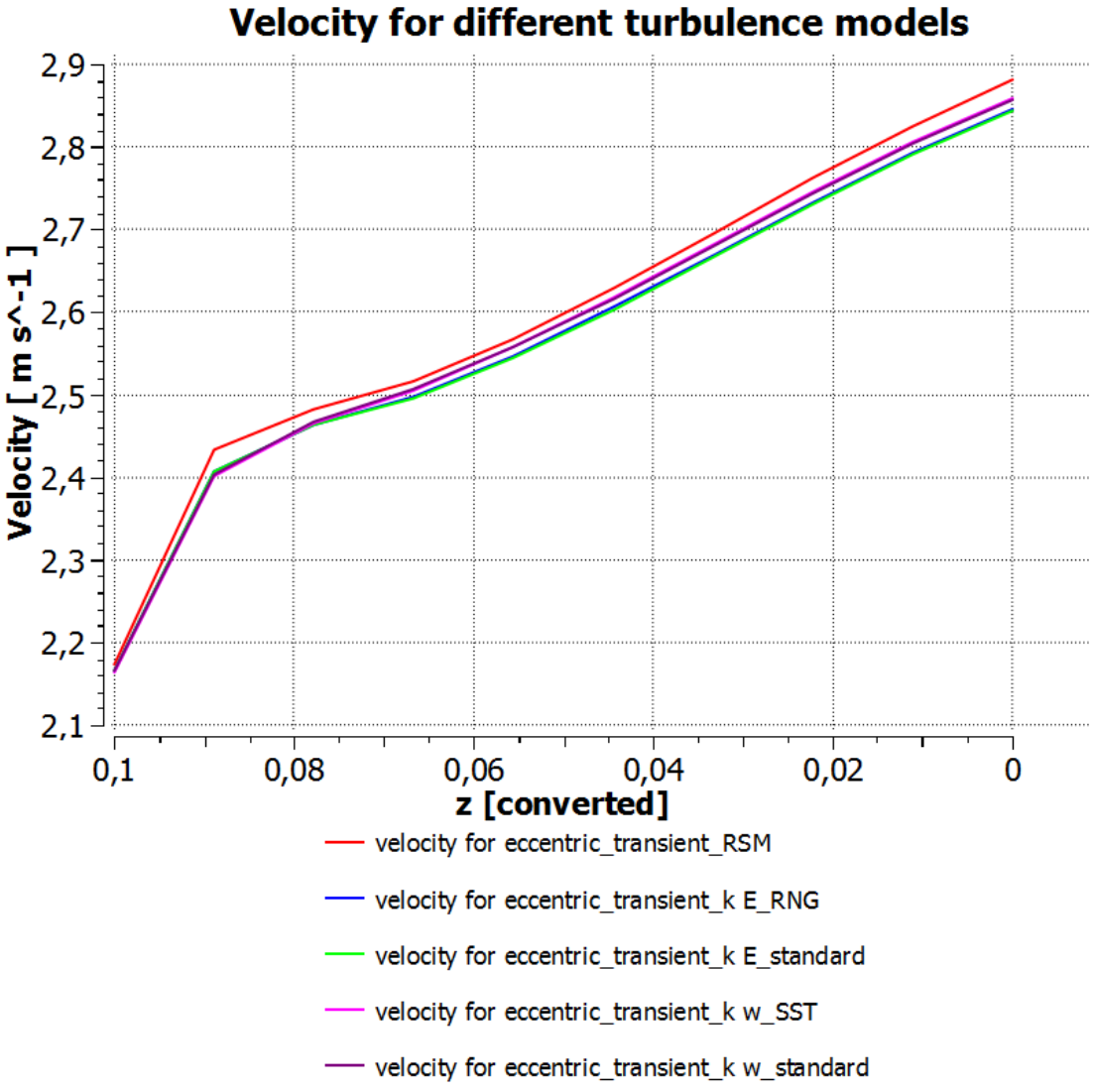

Figure 4-24. Velocity values along the annulus for eccentric assembly in the larger gap for different turbulence models.

The bigger gap of the annulus gives a better space for the flow. It is observed, that the velocity increases along the pipe and, as it was seen in concentric case, reach the highest values on the symmetry plane (outer pipe). Among the investigated models the RSM provides highest results.

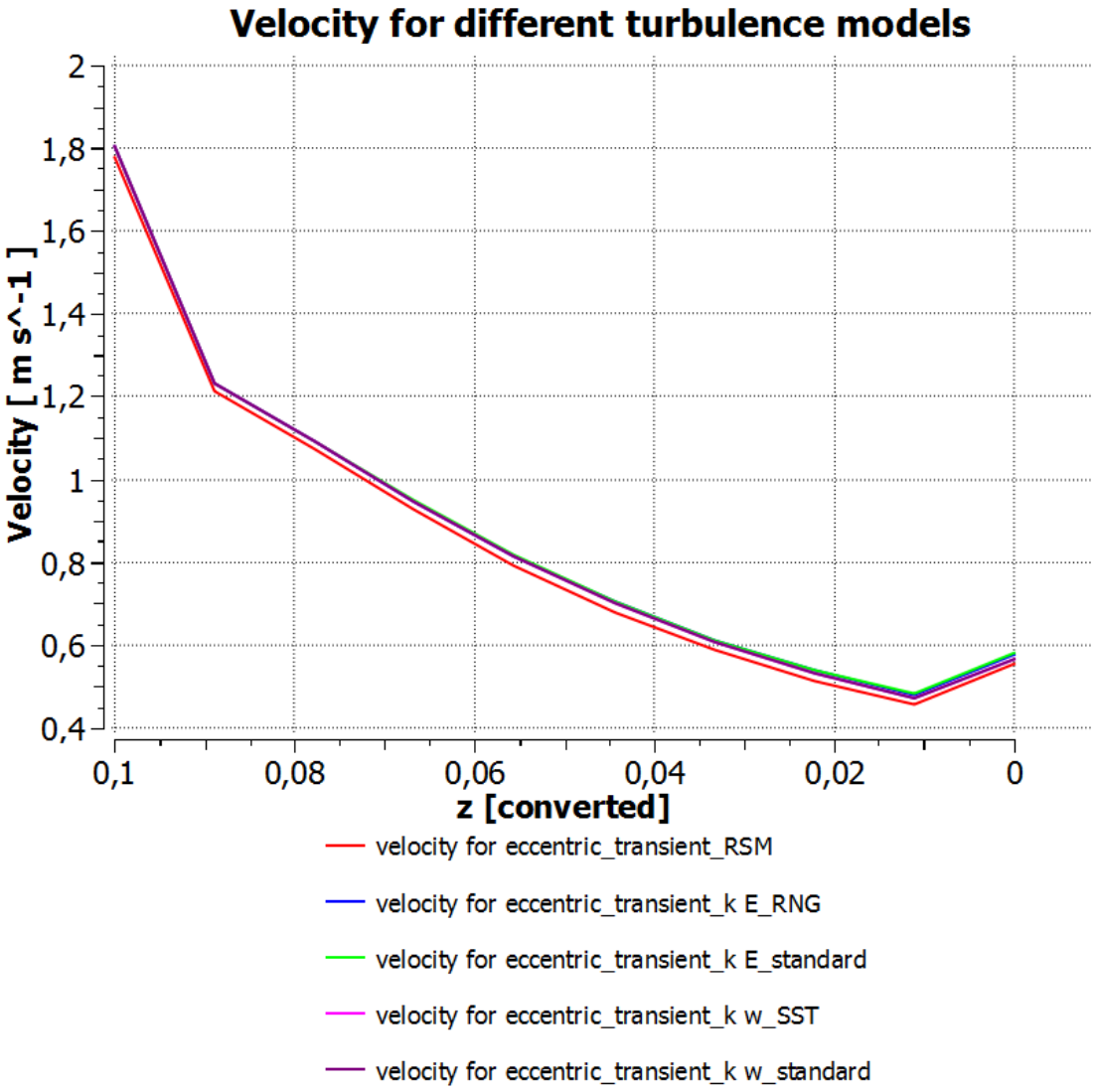

Figure 4-25. Velocity values along the annulus for eccentric assembly in the narrow gap for different turbulence models.

Status of velocity differs on the other side of the annulus where the gap is narrow. Here, the considerable decrease of the velocity is observed moving away from the inlet towards the outflow. The contours of velocity (paragraph 4.3.4.) show, that the values of velocity are the smallest on the outer pipe wall near the thin window. The eccentricity results in low-velocity fluid flow on this side. Same as above, the RSM model obtains reflects higher velocity among other approaches.

4.4.Selection of preferred model for eccentric assembly

Comparing the methodology used in choosing the turbulence approach to project the flow in concentric assembly and eccentric case, the Reynolds stress model here also gives improved results. As described before, it usually fits more complex cases of flows or geometries. The analyzed situation might be considered as one of the above because RSM model stands out among the others, so it would be used for the eccentric case for 'true dimensions'. The heat transfer rate calculated In Ansys for this approach is slightly higher than for the other.

4.5.Concentric assembly of true dimensions

4.5.1. Residuals

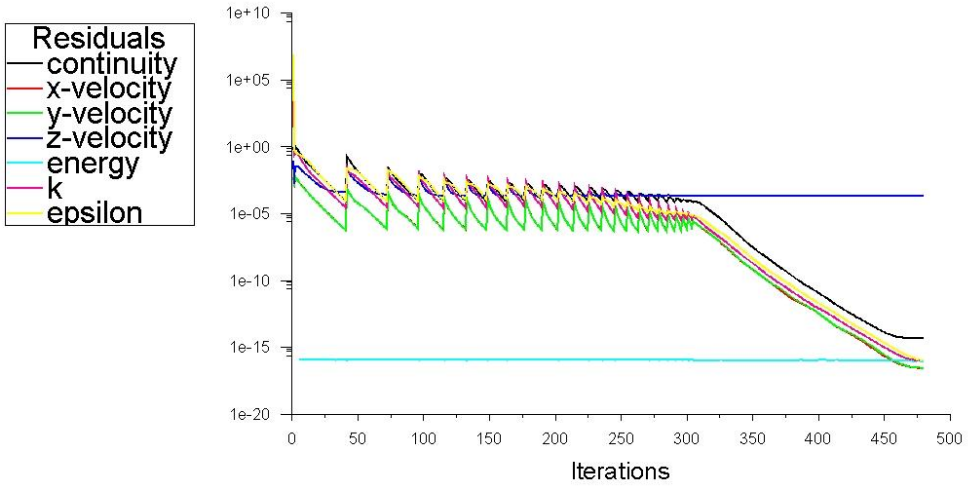

Figure 4-26. Residuals for concentric 'true dimensions' standard K-e model.

Almost all of the residuals of standard K-epsilon model for 'true dimensions' in concentric assembly converged in similar way with rather small differences, but the z-velocity does not follow this path. This could indicate wrong choice of velocity for the case, although the simulation for smaller parameters seemed well prepared.

4.5.2.Streamlines and vortex region

The TKE shown with vortex region after the simulation time also indicates higher values closer to the 'symmetry' (outer pipe) as it was projected in the 'smaller dimensions' case, but here the regions are weaker, on a short-scale.

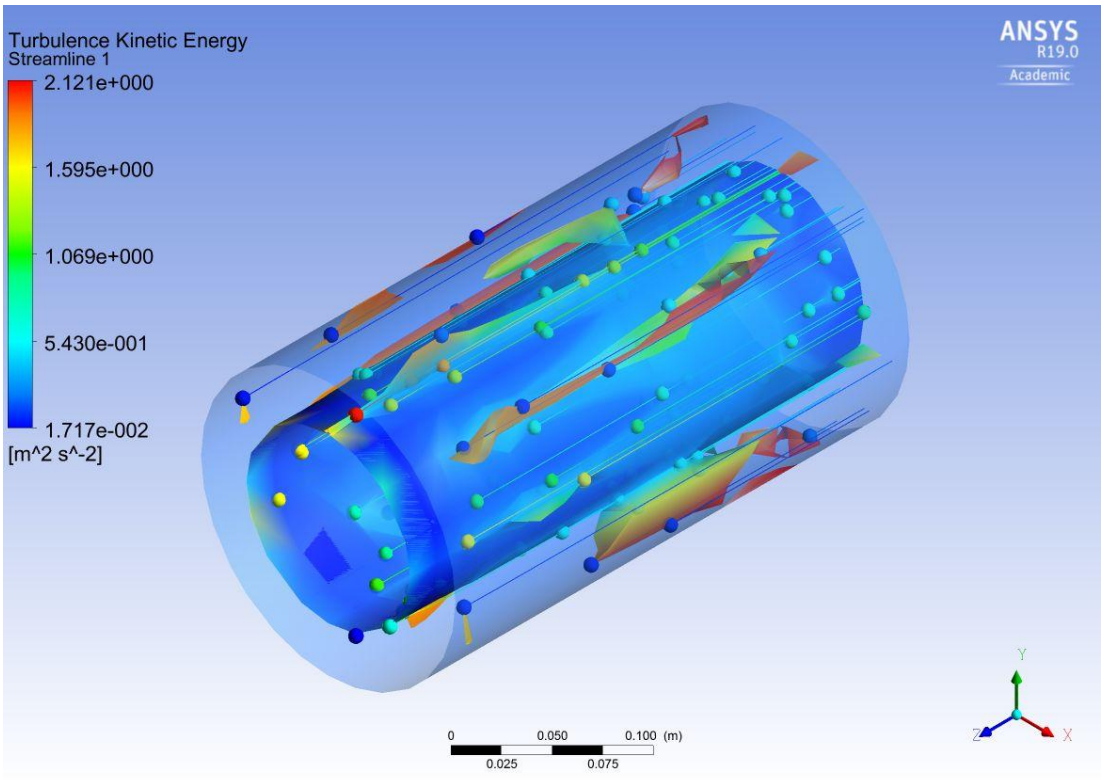

Figure 4-27. Streamlines and vortex regions for concentric 'true dimensions' standard K-e model.

4.5.3.Vectors of pressure

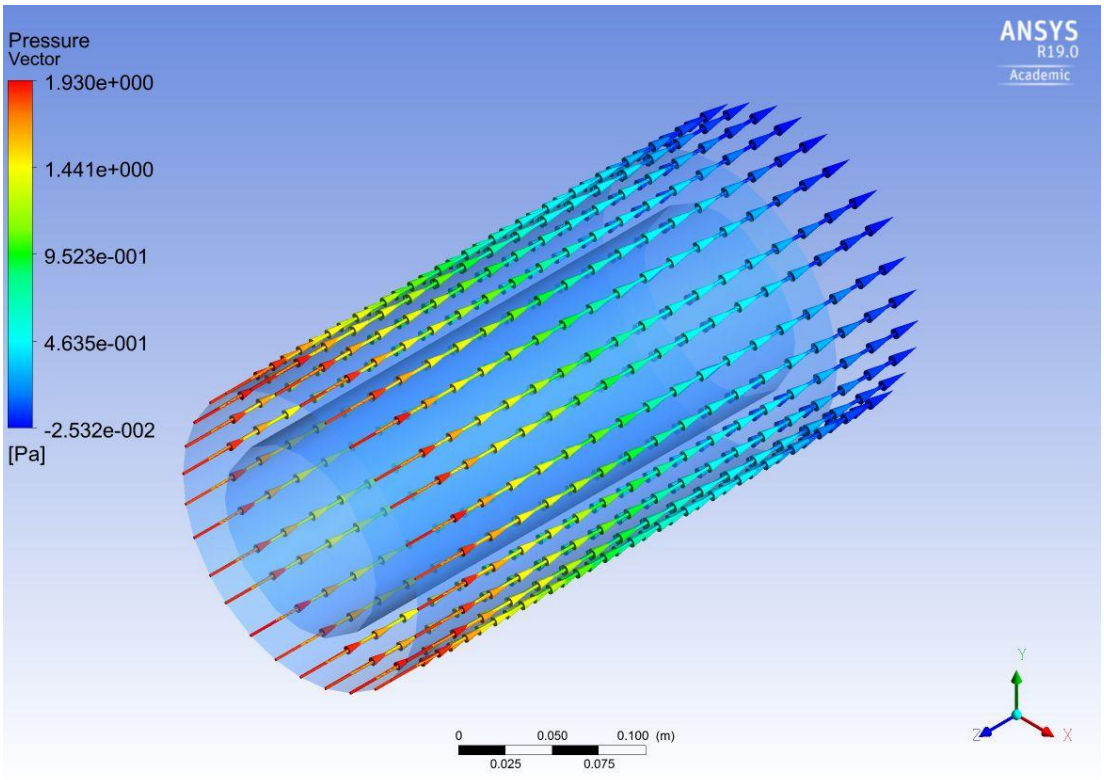

Figure 4-28. Vectors of pressure for concentric 'true dimensions' standard K-e model.

Vectors of pressure almost exactly corresponds to the distribution on ‘small dimensions’. Naturally, the values are slightly higher but the follow the same pattern.

4.5.4.Contours of velocity

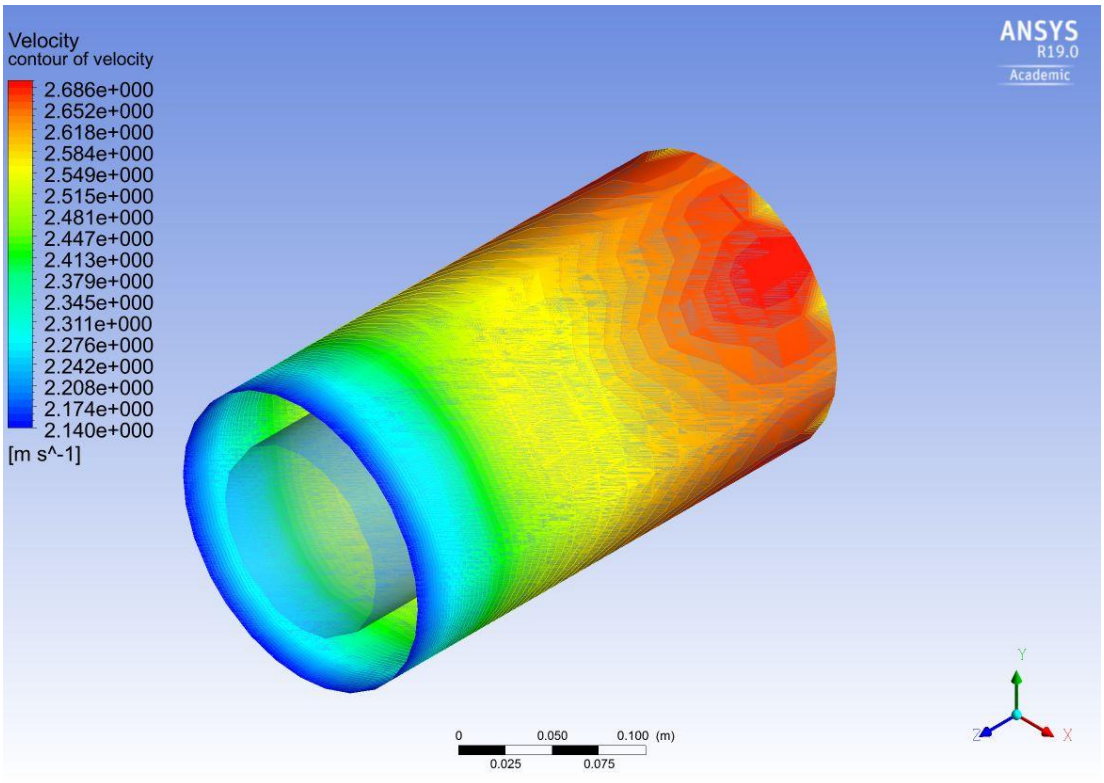

Figure 4-29. Contours of velocity for concentric 'true dimensions' standard K-e model.

As in the case of pressure, the velocity contours over the symmetry of ‘true dimensions’ correlate in the same manner as for ‘small dimensions’. Velocity increases at the end of the pipe, entering the annulus with the input value of 2,14 m/s.

4.5.5.Velocity along the annulus

Velocity in the annulus distributes in the same manner for checked geometry dimensions. Over the ‘wall’ boundary condition (inner pipe) it has small values that visibly increase across the annulus towards the outer pipe, which is set as the ‘symmetry’.

4.6.Eccentric assembly of true dimensions

4.6.1. Residuals

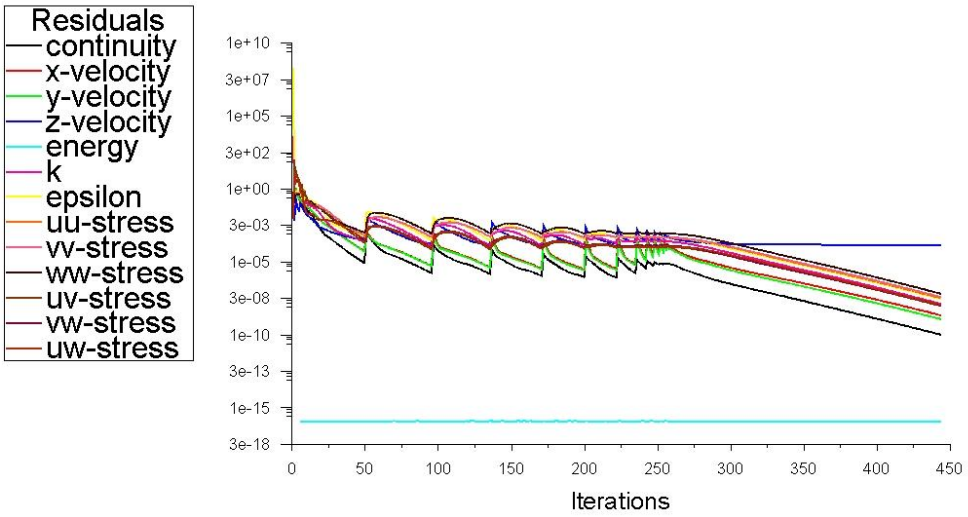

Figure 4-30. Residuals for eccentric 'true dimensions' RSM model.

Residuals for simulation with RSM approach mostly converge for the input value of 0,0001, but with the exception of z-velocity. As it was stated before, the given velocity of 2,14 m/s does not merge with other parameters for this kind of assembly.

4.6.2.Streamlines and vortex region

Vortex generation over the eccentric annulus of 'true dimensions' formulates better results in larger gap of the annulus, same as in the 'small dimensions'. Consistently values of TKE are higher than before. The flow does not rotate around the flow axis in the narrow gap.

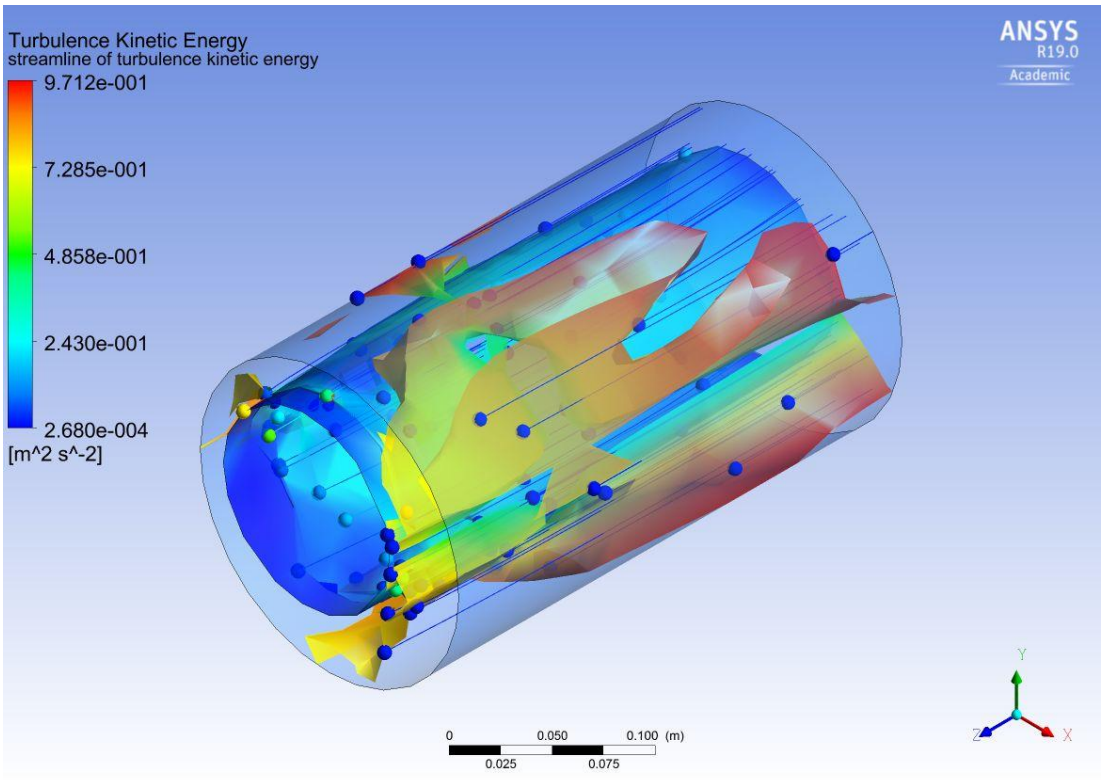

Figure 4-31. Streamlines and vortex regions for eccentric 'true dimensions' RSM model.

4.6.3.Vectors of pressure

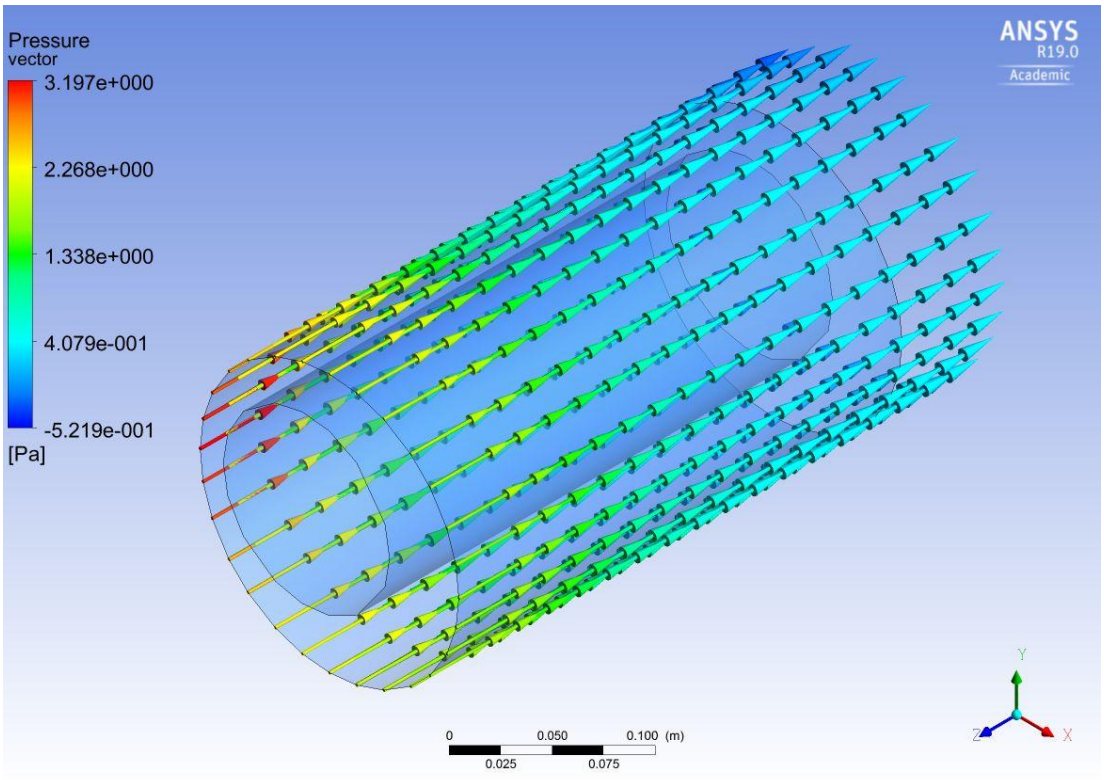

Figure 4-32. Vectors of pressure for eccentric 'true dimensions' RSM model.

Vectors of pressure for RSM models work in the same pattern for ‘small’ and ‘true’ dimensions. They show limited values in the bigger window of the eccentric annulus starting from the velocity inlet and dropping with the flow direction. In the tight gap, pressure gives higher results at the beginning of the flow.

4.6.4.Contours of velocity

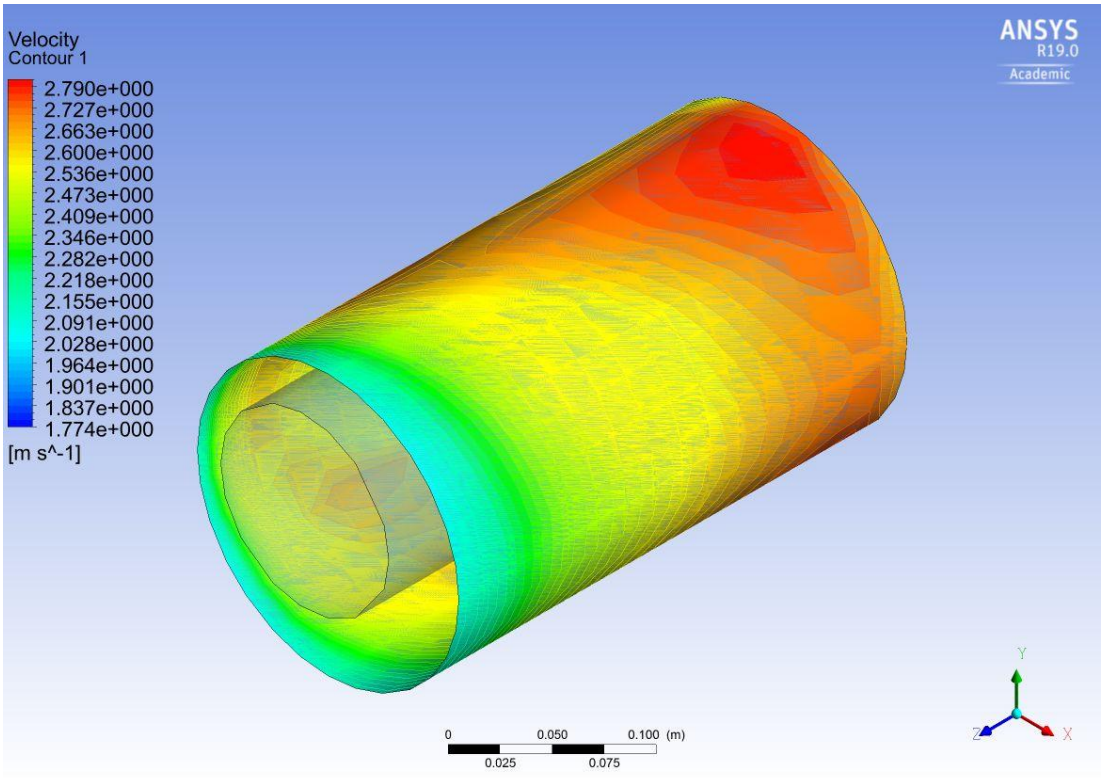

Figure 4-33. Contours of velocity over larger gap for eccentric 'true dimensions' RSM model.

Velocity on the symmetry plane (outer pipe) have larger values near the bigger gap of the annuls, than near the narrow one. It corresponds to the pressure distribution – higher pressure in the small zone is related to lower velocity (as seen on the Figure 4-34.) and higher velocity in the larger gap is associated with the lower pressure. The distribution of those parameters is universal and applies in the ‘small dimensions’ case as well.

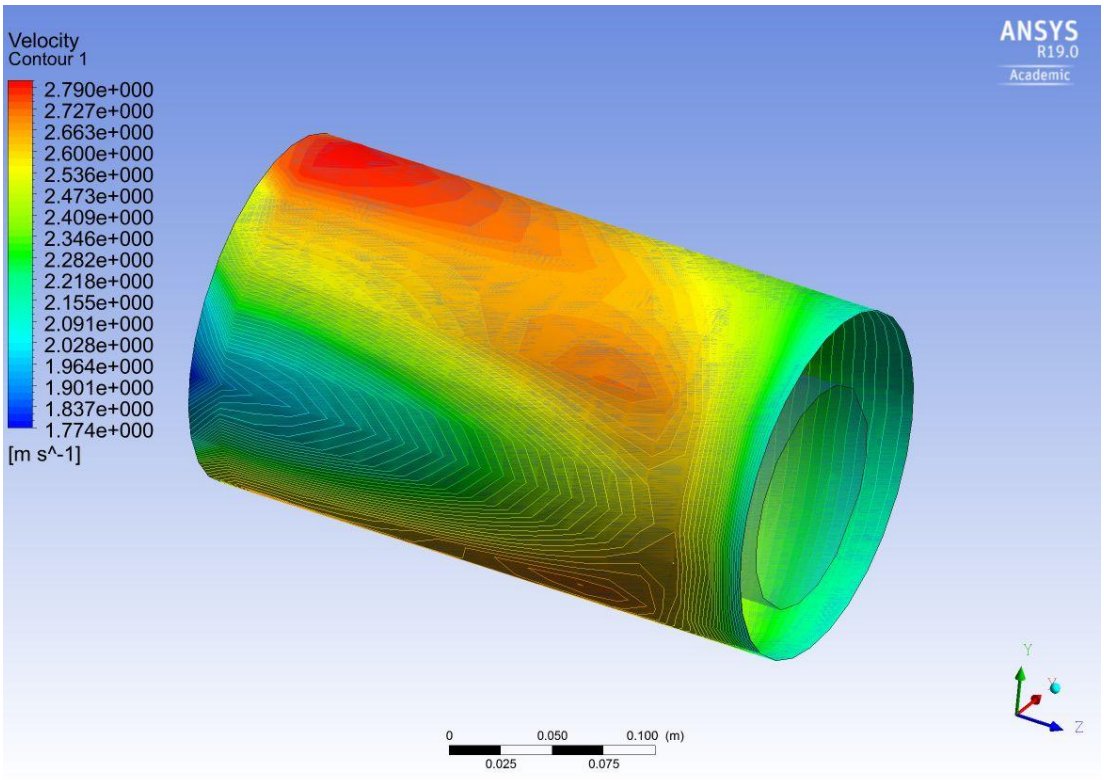

Figure 4-34. Contours of velocity over narrow gap for eccentric 'true dimensions' RSM model.

4.6.5.Velocity along the annulus

Following the previous examples of velocity distribution in the annulus, the 'true dimensions' eccentric case demonstrates analogous behavior. Over the 'wall' boundary (inner pipe) the values are clearly weaker than for the points located further to the outer pipe.

4.7.Change of the materials of pipes

In this example the materials of inner and outer pipes were changed to analyze the difference in heat transfer rate. The boundary condition of simulation for outer pipe was modified to 'wall' to involve the influence of the elements physics. The inner pipe was left with the same status. First material was referred as aluminum and second one as steel. The geometry was set for the 'true dimensions' case of eccentric assembly for RSM turbulence model.

Parameter	Value	Unit
Density	2719	kg/m^3
Specific heat	871	J/kg-K
Thermal conductivity	202,4	W/m-K
Temperature	293,15	K

Table 4-1. Parameters of aluminum set for 'wall' boundary condition.

Parameter	Value	Unit
Density	7850	kg/m^3
Specific heat	490	J/kg-K
Thermal conductivity	54	W/m-K
Temperature	293,15	K

Table 4-2. Parameters of steel set for 'wall' boundary condition.

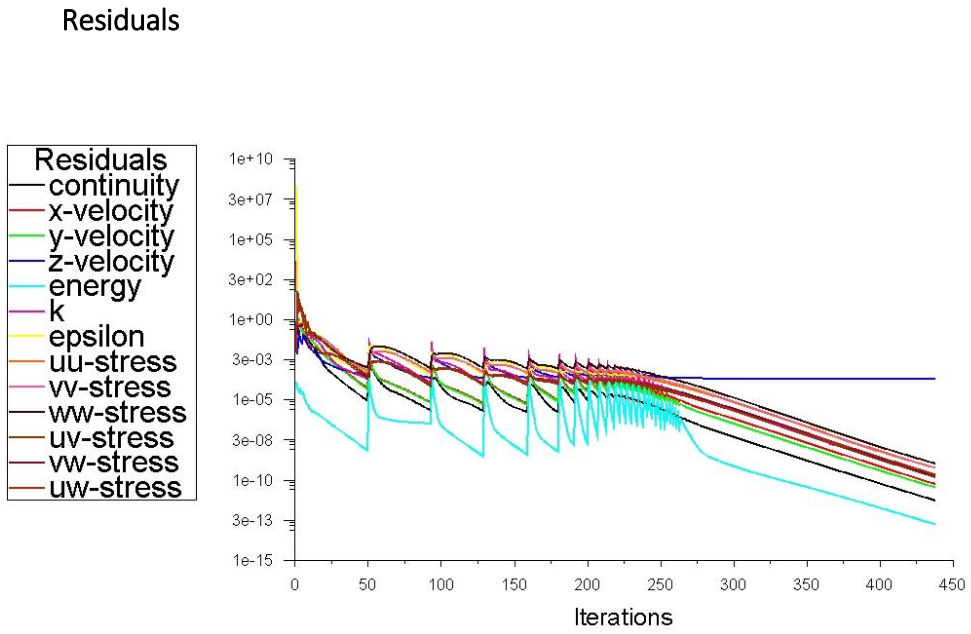

Figure 4-35. Residuals for eccentric 'true dimensions' RSM model of material change.

Unlike the previous cases, adjusting the temperature to particular material of the pipe resolves in the energy variations in the calculation.

4.7.2.Streamlines and vortex regions

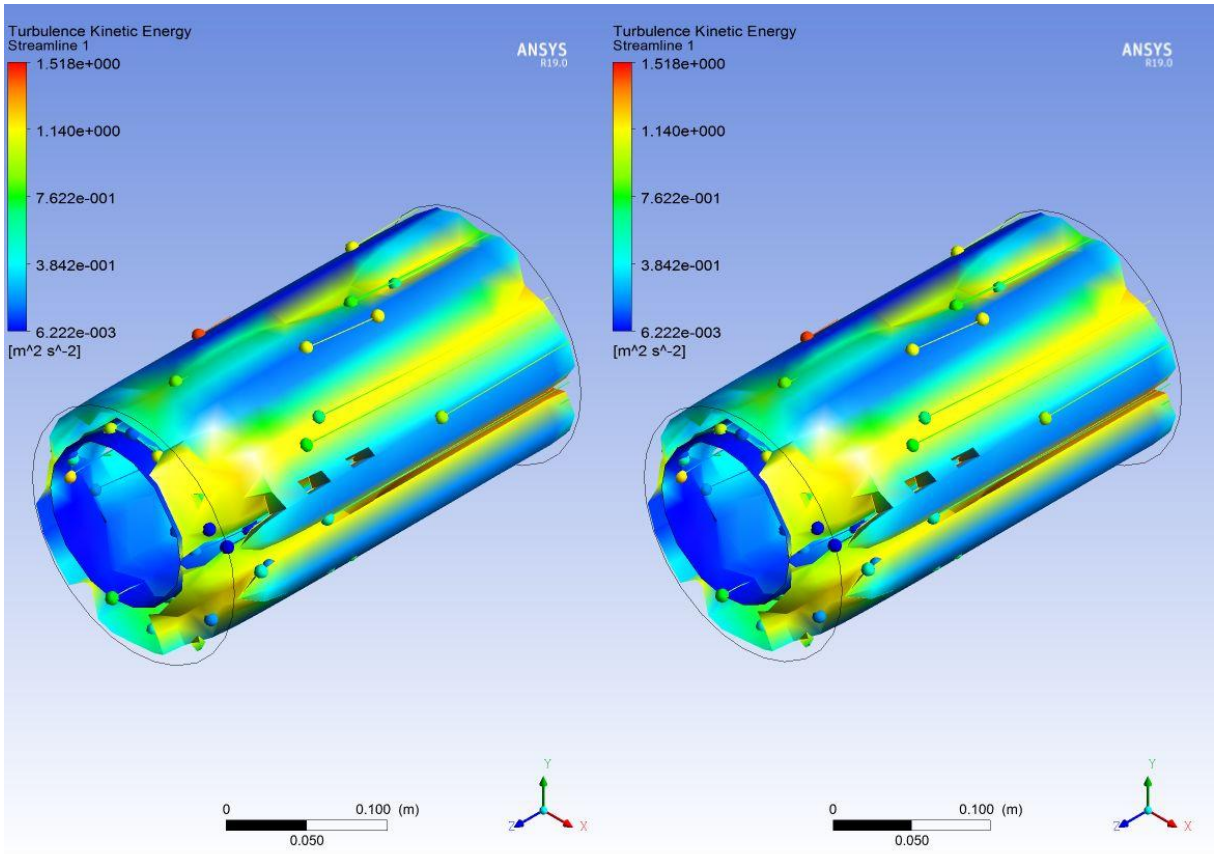

Figure 4-36. Streamlines and vortex regions for eccentric 'true dimensions' for aluminum (left) and steel (right) for RSM model.

Dissimilar to previous examples, vortex regions of velocity and streamlines of TKE indicate the movement covering the whole annulus after the set simulation time.

4.7.3.Contours of velocity and vectors of pressure

Change of the pressure vectors was not observed on the outer pipe. With the boundary condition of ‘wall’ set for this element, the contours of velocity could not be projected here as it does not transmit the flow.

Meanwhile, the contours of velocity could be shown on the outflow plane. Here, the highest values are obtained in the large gap of the annulus, but the results close to walls of outer and inner pipe are much smaller.

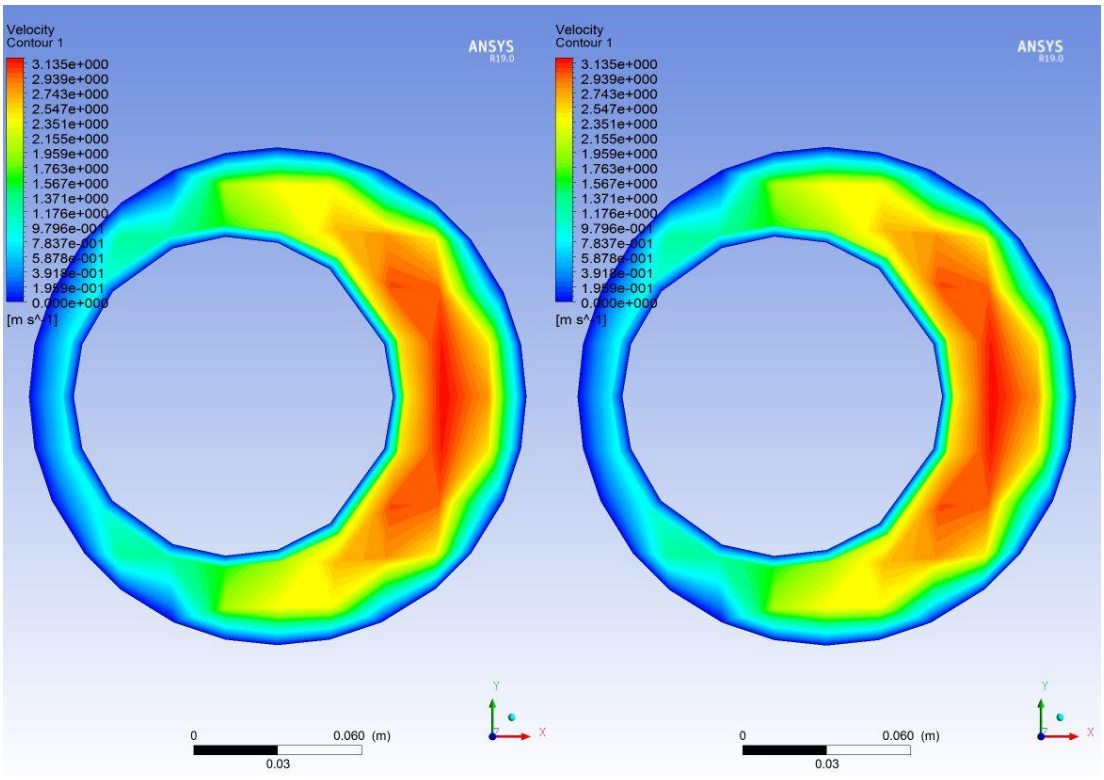

Figure 4-37. Contours of velocity on outflow for eccentric 'true dimensions' case of aluminum (left) and steel (right).

4.7.4.Total heat transfer rate calculation

Material	Heat rate at inlet	Heat rate at outlet	Difference	Unit
Aluminum	0,443	163,701	163,258	Watt
Steel	0,427	161,666	161,239	Watt

Table 4-3. Calculation of heat transfer rate for aluminum and steel.

Above calculation demonstrates the difference of total heat transfer rate between the inlet and outlet of the pipe's assembly. Higher rate for aluminum could be obtained due to the considerably greater values of thermal conductivity of this material, than of steel. This is the main driver for the heat transfer change in real-life examples of particular materials used for the pipes production.

5. Conclusions

In this study several objects were addressed. To analyze the research questions, the geothermal energy needed a proper introduction. As it was highlighted several times, this branch of energy industry has a major potential, but complete investigation on geothermal exploitation brought to the light specific issues existing in this field.

The process of drilling for geothermal resources relates to operations conducted in oil & gas industry. Due to more challenges, like: high concentrations of H_2S, higher thermal stresses and more abrasive rocks resulting in slower ROP, it requires wider financial investments. Moreover, the integrity of the wells demands great concerns. Further, this project elaborates on a problem of heat transfer. It gives an overview on how complex is this matter. The situation is mostly referred as a multi-phase concern with multiple individual properties. Crucial part of the numerical investigation is addressing the geothermal exploitation governing equations of mass energy balance, momentum balance and energy balance.

Examination of flows in concentric and eccentric annuli exposed the influence of geometry arrangement on the medium transfer along them. The assembly affects the values of every final parameter investigated in the simulation, despite the exact input specifications.

Furthermore, the application of five turbulence models show the substantial contrast of results depending on each approach. In some cases, as the core model is the same, supplementary equations do not expose major differences. In addition, rather simple elements with uncomplicated flow of single-phase working fluid not necessarily require complex, higher-level turbulence closure to fulfill the objective of the most effective flow.

The change of the materials of inner and outer pipes influences the total heat transfer in the annulus. The governing parameter of this modification is the thermal conductivity of the element.

6. References

Augustine, C., Tester, J. W., Anderson, B., Petty, S., & Livesay, B. (2006). *A comparison of geothermal with oil and gas well drilling costs.* Paper presented at the Proceedings of the 31st Workshop on Geothermal Reservoir Engineering.

Bahiraei, M., Rahmani, R., Yaghoobi, A., Khodabandeh, E., Mashayekhi, R., & Amani, M. (2018). Recent research contributions concerning use of nanofluids in heat exchangers: A critical review. *Applied Thermal Engineering*.

Bergman, T. L., Incropera, F. P., DeWitt, D. P., & Lavine, A. S. (2011). *Fundamentals of heat and mass transfer*: John Wiley & Sons.

Bicalho, I., dos Santos, D., Ataíde, C., & Duarte, C. (2016). Fluid-dynamic behavior of flow in partially obstructed concentric and eccentric annuli with orbital motion. *Journal of Petroleum Science and Engineering, 137*, 202-213.

Brooks, R., & Corey, T. (1964). Hydraulic Properties Of Porous Media. *Hydrology Papers, Colorado State University, 24*.

Brownell, D., Garg, S., & Pritchett, J. (1977). Governing equations for geothermal reservoirs. *Water Resources Research, 13*(6), 929-934.

Busch, A., Islam, A., Martins, D. W., Iversen, F. P., Khatibi, M., Johansen, S. T., . . . Meese, E. A. (2018). Cuttings-Transport Modeling–Part 1: Specification of Benchmark Parameters with a Norwegian-Continental-Shelf Perspective. *SPE Drilling & Completion*.

Carden, R. S., Nicholson, R., Pettitt, R., & Rowley, J. (1983). *Unique aspects of drilling and completing hot-dry-rock geothermal wells*. Retrieved from

Carr-Cornish, S., & Romanach, L. (2014). Differences in public perceptions of geothermal energy technology in Australia. *Energies, 7*(3), 1555-1575.

Chung, S. Y., Rhee, G. H., & Sung, H. J. (2002). Direct numerical simulation of turbulent concentric annular pipe flow: Part 1: Flow field. *International Journal of Heat and Fluid Flow, 23*(4), 426-440.

Chung, S. Y., & Sung, H. J. (2003). Direct numerical simulation of turbulent concentric annular pipe flow: Part 2: Heat transfer. *International Journal of Heat and Fluid Flow, 24*(3), 399-411.

Davidson, L. (2017). An Introduction to Turbulence Models. *Department of Thermo and Fluid Dynamics, Chalmers University of Technology Göteborg, Sweden*.

Dickson, M. H., & Fanelli, M. (2004). What is geothermal energy. *International Geothermal Association, Pisa, Italy*.

Diglio, G., Roselli, C., Sasso, M., & Channabasappa, U. J. (2018). Borehole heat exchanger with nanofluids as heat carrier. *Geothermics, 72*, 112-123.

DiPippo, R. (2016). *Geothermal Power Generation: Developments and Innovation*: Woodhead Publishing.

Estrada, E., Labat, M., Lorente, S., & Rocha, L. A. (2018). The impact of latent heat exchanges on the design of earth air heat exchangers. *Applied Thermal Engineering, 129*, 306-317.

Franco, A., & Vaccaro, M. (2014). Numerical simulation of geothermal reservoirs for the sustainable design of energy plants: a review. *Renewable and Sustainable Energy Reviews, 30*, 987-1002.

Gallup, D. L. (2009). Production engineering in geothermal technology: a review. *Geothermics, 38*(3), 326-334.

Ganguly, S., & Kumar, M. M. (2012). Geothermal reservoirs—A brief review. *Journal of the*

Geological Society of India, 79(6), 589-602.
Ganguly, S., & Kumar, M. M. (2014). Analytical solutions for transient temperature distribution in a geothermal reservoir due to cold water injection. *Hydrogeology Journal, 22*(2), 351-369.
Hasan, A., & Kabir, C. (1991). *Heat transfer during two-Phase flow in Wellbores; Part I--formation temperature.* Paper presented at the SPE Annual Technical Conference and Exhibition.
Heberle, F., & Brüggemann, D. (2014). Thermoeconomic analysis of hybrid power plant concepts for geothermal combined heat and power generation. *Energies, 7*(7), 4482-4497.
Hochstein, M. (1990). Classification and assessment of geothermal resources. *Small geothermal resources: A guide to development and utilization, UNITAR, New York*, 31-57.
Holman, J. (2006). Heat Transfer, Mc Grow-Hill. *Inc., New York*.
Ikenwilo, O., Smith, L., Cornelissen, H., & Magraw, R. (2016). *Geothermal Well Integrity Study*. Retrieved from
Ipek, G., Smith, J., & Bassiouni, Z. (2002). *Estimation of underground blowout magnitude using temperature logs.* Paper presented at the SPE Annual Technical Conference and Exhibition.
Kaldal, G. S., Jonsson, M., Palsson, H., & Karlsdottir, S. (2015). Structural modeling of the casings in high temperature geothermal wells. *Geothermics, 55*, 126-137. doi:https://doi.org/10.1016/j.geothermics.2015.02.003
Kayabasi, E., & Kurt, H. (2018). Simulation of heat exchangers and heat exchanger networks with an economic aspect. *Engineering Science and Technology, an International Journal, 21*(1), 70-76.
Kumar, V., Saini, S., Sharma, M., & Nigam, K. (2006). Pressure drop and heat transfer study in tube-in-tube helical heat exchanger. *Chemical Engineering Science, 61*(13), 4403-4416.
Lentsch, D., Dorsch, K., Sonnleitner, N., & Schubert, A. (2015). Prevention of casing failures in ultra-deep geothermal wells (Germany). *Prevention, 19*, 25.
LeVeque, R. J. (2002). *Finite volume methods for hyperbolic problems* (Vol. 31): Cambridge university press Cambridge.
Lohne, H. P., Ford, E. P., & Mansouri, M. (2016). *Well integrity risk assessment in geothermal wells–Status of today*. Retrieved from
Mercer Jr, J. W., Faust, C., & Pinder, G. (1974). *Geothermal reservoir simulation*. Retrieved from
Neto, J., Martins, A., Ataíde, C., & Barrozo, M. (2014). The effect of the inner cylinder rotation on the fluid dynamics of non-Newtonian fluids in concentric and eccentric annuli. *Brazilian Journal of Chemical Engineering, 31*(4), 829-838.
Neto, J., Martins, A., Neto, A. S., Ataíde, C., & Barrozo, M. (2011). CFD applied to turbulent flows in concentric and eccentric annuli with inner shaft rotation. *THE CANADIAN JOURNAL OF CHEMICAL ENGINEERING, 89*(4), 636-646.
Nouri, J., Umur, H., & Whitelaw, J. (1993). Flow of Newtonian and non-Newtonian fluids in concentric and eccentric annuli. *Journal of Fluid Mechanics, 253*, 617-641.
Nouri, J., & Whitelaw, J. (1997). Flow of Newtonian and non-Newtonian fluids in an eccentric annulus with rotation of the inner cylinder. *International Journal of Heat and Fluid Flow, 18*(2), 236-246.
Olasolo, P., Juárez, M., Morales, M., & Liarte, I. (2016). Enhanced geothermal systems (EGS): A

review. *Renewable and Sustainable Energy Reviews, 56*, 133-144.
O'Sullivan, M. J., Pruess, K., & Lippmann, M. J. (2001). State of the art of geothermal reservoir simulation. *Geothermics, 30*(4), 395-429.
Pan, C., Chávez, O., Romero, C. E., Levy, E. K., Corona, A. A., & Rubio-Maya, C. (2016). Heat mining assessment for geothermal reservoirs in Mexico using supercritical CO2 injection. *Energy, 102*, 148-160.
Patankar, S. (1980). *Numerical heat transfer and fluid flow*: CRC press.
Pereira, F., Barrozo, M., & Ataíde, C. (2007). CFD predictions of drilling fluid velocity and pressure profiles in laminar helical flow. *Brazilian Journal of Chemical Engineering, 24*(4), 587-595.
Petrică, V. C. (2016). Common geothermal well design and a case study of the low-temperature geothermal reservoir in Otopeni, Romania.
Rapantova, N., Pospisil, P., Koziorek, J., Vojcinak, P., Grycz, D., & Rozehnal, Z. (2016). Optimisation of experimental operation of borehole thermal energy storage. *Applied Energy, 181*, 464-476.
Saha, S., Chin, C., Blackburn, H., & Ooi, A. (2011). The influence of pipe length on thermal statistics computed from DNS of turbulent heat transfer. *International Journal of Heat and Fluid Flow, 32*(6), 1083-1097.
Sanyal, S. K. (2005). *Classification of geothermal systems–a possible scheme.* Paper presented at the Thirtieth Workshop on Geothermal Reservoir Engineering, Stanford University, Stanford, California.
Serpen, U., & Başel, E. D. K. (2015). *Optimization of Geothermal Borehole Diameters*. Paper presented at the World Geothermal Congress 2015, Melbourne, Australia.
Shi, Y., Song, X., Li, G., Yang, R., Shen, Z., & Lyu, Z. (2018). Numerical investigation on the reservoir heat production capacity of a downhole heat exchanger geothermal system. *Geothermics, 72*, 163-169.
Sodja, J. (2007). Turbulence models in CFD. *University of Ljubljana*, 1-18.
Sun, X., Wang, K., Yan, T., Shao, S., & Jiao, J. (2014). Effect of drill-pipe rotation on cuttings transport using computational fluid dynamics (CFD) in complex structure wells. *Journal of Petroleum Exploration and Production Technology, 4*(3), 255-261.
Teodoriu, C., & Falcone, G. (2009). Comparing completion design in hydrocarbon and geothermal wells: The need to evaluate the integrity of casing connections subject to thermal stresses. *Geothermics, 38*(2), 238-246.
Thorsteinsson, H., Augustine, C., Anderson, B., Moore, M., & Tester, J. (2008). *The impacts of drilling and reservoir technology advances on EGS exploitation.* Paper presented at the Proceedings, Thirty-Third Workshop on Geothermal Reservoir Engineering, Institute for Sustainable Energy, Environment, and Economy (ISEEE).
Þórhallsson, S. (2012). *Common problems faced in geothermal generation and how to deal with them*. Paper presented at the Short Course on Geothermal Drilling, Resource Development and Power Plants, Santa Tecla, El Salvador.
Toth, A., & Bobok, E. (2016). *Flow and Heat Transfer in Geothermal Systems: Basic Equations for Describing and Modeling Geothermal Phenomena and Technologies*: Elsevier.
Vasini, E. M., Battistelli, A., Berry, P., Bonduà, S., Bortolotti, V., Cormio, C., & Pan, L. (2017). Interpretation of production tests in geothermal wells with T2Well-EWASG. *Geothermics*.
Wanner, C., Eichinger, F., Jahrfeld, T., & Diamond, L. W. (2017). Unraveling the formation of large amounts of calcite scaling in geothermal wells in the Bavarian Molasse Basin: a

reactive transport modeling approach. *Procedia earth and planetary science, 17*, 344-347.
White, D., Muffler, L., & Truesdell, A. (1971). Vapor-dominated hydrothermal systems compared with hot-water systems. *Economic Geology, 66*(1), 75-97.
Williams, C. F., Reed, M. J., & Anderson, A. F. (2011). *Updating the classification of geothermal resources.* Paper presented at the Proceedings, Thirty-Sixth Workshop on Geothermal Reservoir Engineering.
Witherspoon, P., Neuman, S., Sorey, M., & Lippmann, M. (1975). Modeling geothermal systems.
Younger, P. L. (2014). *Energy: All that Matters*: Hachette UK.
Younger, P. L. (2015). Geothermal energy: delivering on the global potential. In: Multidisciplinary Digital Publishing Institute.
Zhou, F., & Zheng, X. (2015). Heat transfer in tubing-casing annulus during production process of geothermal systems. *Journal of Earth Science, 26*(1), 116-123.